USING TIRE DERIVED AGGREGATES BACKFILLING ALTERNATIVES FOR RETAINING WALL STRUCTURES

by

Aiyleen Elsa Ravi

Submitted in partial fulfilment of the requirements for the degree of
Master of Applied Science

at

Dalhousie University
Halifax, Nova Scotia
August 2024

Dalhousie University is located in Mi'kma'ki, the
Ancestral and unceded territory of the Mi'kmaq.
We are all Treaty people.

TABLE OF CONTENTS

LIST OF TABLES

LIST OF FIGURES

ABSTRACT

Around one billion tires reach their useful life every year worldwide. Thus, its important to manage scrap tires that goes to landfill sites, where they put our environment and health at risk. Many tire recycling programs were done, where scrap tires were collected and recycled into various products. Tire derived aggregate (TDA) is one such product. Its lightweight and free draining properties makes it suitable to replace conventional fill material by reducing forces between embankments, retaining walls, bridge abutments and landfill areas.

This paper focuses on using TDA as a backfill for retaining wall. The purpose of this study is to reduce the earth pressure on the retaining wall by replacing the conventional soil backfill by tire derived aggregates. A Plaxis 2D finite element model has been developed to investigate the effect of TDA as a backfill material for retaining wall, which was verified against the field measurements. In the analysis, a linear elastic model is adopted for concrete, a Mohr-coulomb model for soil and TDA is designed as a hardening soil model. Furthermore, parametric studies were conducted to examine the earth pressure on retaining wall at different backfill slope angles, and subcases were considered by varying the width of backfill TDA layer in each case of slope angle. The study showed that varying the backfill slope angle have only negligible effect on the results. It was also found that varying the width of backfill TDA layer significantly reduces the earth pressure on the retaining wall.

LIST OF ABBREVIATIONS AND SYMBOLS USED

Abbreviations

RW	Retaining Wall
TDA	Tire Derived Aggregate
FEM	Finite Element Model
2D	Two Dimensional
ANSYS	Analysis System
Auto CAD	Automatic Computer Aided Design
FEA	Finite Element Analysis
MSE	Mechanically Stabilized Earth
IBC	International Building Code
ACI	American Concrete Institute
CEN	European Committe for Standardization
EC7	Eurocode 7
ENs	European Normative Standards
BSs	British Standards
BSI	British Standards Institution
SLS	Serviceability Limit State
Das	Design Approaches
BIS	Bureau of Indian Standards
IS	Indian Standards
PVC	Poly Vinyl Chloride
SBC	Safe Bearing Capacity
MCL	Maximum Contaminant Level
LVDT	Linear Variable Differential Transformers
3D	Three Dimensional
RCA	Recycled Concrete Aggregate
CBR	California Bearing Ratio

RLT	Repeated Load Triaxial Test
CED	Cumulative Energy Demand
GWP	Global Warming Potential
AP	Acidification Potential
HS	Hardening Soil
GWT	Ground Water Table

Symbols

%	Percentage
k_p	Coefficient of passive earth pressure
k_a	Coefficient of active earth pressure
E	Elastic modulus
γ	Unit weight
k_o	Coefficient of earth pressure at rest
ν’	Poisson’s ratio
σ_v’	Effective vertical stress
σ_h’	Effective horizontal stress
σ’	Effective stress
c’	Cohesion
ϕ	Angle of internal friction
m	Power
Ɛ	Strain rate
M	Material stiffness matrix
G	Shear modulus
K	Bulk modulus
γ_{unsat}	Unsaturated unit weight
γ_{sat}	Saturated unit weight
E_{50}^{ref}	Reference stiffness modulus
E_{oed}^{ref}	Oedometer stiffness modulus

E_{ur}^{ref}	Unloading-reloading modulus
Ψ	Dilatancy angle
P^{ref}	Reference confining pressure
ε_1	Vertical strain
q'	Deviatoric stress
H	Height
BW	Base width
T	Thickness

ACKNOWLEDGEMENTS

I begin by expressing my deepest gratitude to ALMIGHTY GOD, who has guided and supported me throughout this research journey. His divine grace and wisdom have enabled me to complete this thesis.

I would like to extend my profound gratitude and sincere appreciation to my respected supervisor Dr. Hany El Naggar, for his expert guidance and unwavering support. I would also like to thank him for his empathy, patience and encouragement throughout my research. It was a great privilege and honor to work and study under his guidance.

I am extremely grateful to my parents, for their love, prayers and support during my journey. I am very much thankful to my brother for his love and understanding. Also, I express my sincere gratitude to all my friends for all their support and encouragement.

I am grateful for the collective efforts and support of all these individuals, without which this research would not have been possible.

CHAPTER 1 INTRODUCTION

1.1 Research Background

Retaining walls have been a crucial element in infrastructure for thousands of years, playing a vital role in shaping our built environment. From ancient civilizations to present day, retaining walls have been used to retain earth or other material, to maintain the ground surface at different elevations on either side of the wall, to harness the power of water, limit soil erosion and to produce usable land.

At any place if soils are unstable, steep slopes are there, or heavy runoff is present, retaining walls are used to stop erosion. Excessive runoff can wash out roadways and structures and protecting sediment runoff is a big environmental and water quality consideration in transportation projects like road and bridge projects. In these scenarios constructing retaining walls, reduces removal of vegetation and reduction in erosion caused by runoff (Diwalkar,2020).

There are generally two classifications of retaining walls: externally stabilized walls which use heavy materials on the outside of the soil mass to resist soil movement, and internally stabilized walls which utilize artificial reinforcements placed in the soil to carry tensile loads and stabilize the soil mass. Gravity walls, reinforced concrete counterfort walls and reinforced concrete cantilever walls are typical examples of externally stabilized retaining walls. Metal strip walls, anchored earth walls and geotextile reinforced walls are typical examples of internally stabilized retaining walls (Khan and Sikder, 2004).

The earth forces acting on the retaining wall due to backfill are a major problem in practical design, and thus it is critical to calculate the thrust on the wall precisely, allowing the assessment of the wall's safety during its operation time. Coulomb or Rankine Earth pressures theory based on limit equilibrium analysis could be used to calculate the forces exerted on the wall. Over the years, retaining walls have evolved considerable advances in materials, design and building processes transforming them into complex structures that requires careful engineering applications. Figure 1.1 shows an example of a retaining wall used for highways.

Fig 1.1 An example of a Retaining wall used for highways (Redi-Rock K.I.T)

1.2 Backfilling of Retaining Wall

The construction of a retaining wall involves careful planning, design, and execution to ensure stability, safety, and durability. Backfilling is a crucial process in the construction of RW that involves filling the excavated areas around the retaining wall with suitable materials as it serve purposes like, providing support to the structure, helps in transferring loads from the wall to the surrounding soil, promotes proper drainage, prevents water infiltration, prevent soil erosion and settlement, reduces pressure on the wall and enhances overall wall stability.

The choice of suitable backfill material depends on the specific project requirements, site conditions and design considerations. Granular, coarse-grained soils are highly permeable and are the preferred backfill soils of gravity walls. The coarse grains and large void spaces allow the excess pore-water pressure to dissipate quickly, which results in the drained condition and decreases the stresses imposed on the retaining wall. The drained condition arises when water within the soil can dissipate and only the soil particles support loads. Conversely, soils in the undrained condition retain water within the soil and both soil particles and water must contribute to supporting stresses. The existence of either the drained or undrained conditions depends on soil type, grain size distribution, geological formation, rate of loading and artificial drainage systems within the soil (Budhu, 2007).

Furthermore, aggregates like gravel, crushed stone, TDA, geosynthetic materials like geogrids, geotextiles, geo-composites and various recycled materials like recycled concrete aggregate, asphalt, glass are also widely used for backfilling retaining wall.

1.3 Lateral Earth Pressure

Along with the self-weight, earth pressure is the majorly acting force for analysis and design of the retaining wall. Cohesive strength of soil and angle of internal friction are very important factors on which the lateral earth pressure depends. Earth pressures distribution is generally triangular, minimum at top of the wall and increasing towards the bottom of wall. This push force can either overturn or push forward the wall if not properly analyzed (Diwalkar,2020).

Lateral earth pressure acts in the horizontal plane in the backfill. Because a retaining wall prevents movement of a soil mass, the wall must provide equal and opposite stresses to counteract the stresses from the soil. In the plane strain condition only the vertical effective stress (σ_v') and horizontal effective stress (σ_h') are considered. The horizontal stress is known as lateral earth pressure and is defined as the magnitude of stresses between the soil mass and the adjoining retaining wall in the horizontal plane. The Lateral Earth Pressure Coefficient, K, is used in calculation of lateral earth pressure and can be applied in three categories: at-rest, passive, and active. Active refers to the wall tilting out away from the soil mass and passive refers to the wall tilting in toward the soil mass (Craig, 1992).

1.4 Innovation in Retaining Wall Construction

In the realm of civil engineering, innovation is the bridge between functional necessity and environmental stewardship. Engineers are increasingly turning to renewable materials, such as recycled concrete, tires and plastic, reducing the environmental

footprint of construction. These innovative approaches showcase the future of retaining wall design, a future where walls not only serve their primary function but also contribute positively to the environment and society by integrating sustainability and technology (Longinos and Widlund, 2022).

Worldwide around one billion tires reach their end of useful life every year. So, its important to manage these scrap tires in an environmentally responsible and productive manner. Re-use of scrap tires in civil engineering applications is essential step in creating a sustainable future. In some situations, use of Tire-Derived Aggregate (TDA) may provide greater economy than those materials traditionally used. Various researchers have carried out investigations on the usage of scrap tire derived materials in civil engineering applications like, fill material in retaining wall backfill (Reddy and Krishna, 2015). In comparison to conventional backfill materials, TDA is distinct mainly because of its lightweight properties, durability, stability and vibration damping characteristics.

This thesis focuses on the investigation of tire derived aggregate as a sustainable and effective backfill material for retaining wall, with a specific emphasis on its ability to reduce earth pressure of the retaining wall. Through a comprehensive review of existing literature and computational simulations, this research aims to provide an in-depth understanding of TDA's potential as backfill material and thus paving the way for a new generation of retaining wall systems that combine innovation, sustainability and performance.

1.5 Computational Analysis

The construction industry has undergone a significant transformation with the advent of computer software applications. PLAXIS 2D is a finite element software that offers unparalleled accuracy and efficiency in geotechnical analysis and design. This study investigates the performance of Tire-Derived Aggregate (TDA) as a backfill material in retaining wall using computational analysis with PLAXIS 2D software. PLAXIS allows for a detailed modeling of the retaining wall backfilled with TDA, enabling accurate simulation of the structural behavior, it also provides detailed stress distributions, enabling designers to identify potential factors to optimize the design, to ensure structural safety, reduce construction costs, thereby revolutionizing the field of geotechnical engineering.

1.6 Research Objectives

This research aims to investigate the effect of TDA as a backfill material for retaining wall under static conditions. The key objectives of the study presented in this thesis are as follows:

- Investigate a field test experiment on retaining wall backfilled with TDA using computational analysis.
- Develop a computational Finite Element Model (FEM), using PLAXIS 2D software to simulate the behaviour of TDA backfilled retaining wall, and to verify the earth pressure in the retaining wall against the existing field data.

- Compare the computational model results with field test data, to evaluate the accuracy and reliability of the model.
- Utilize the validated computational model to conduct parametric studies to investigate the changes in earth pressure under various conditions.

1.7 Thesis Outline

The structure of this thesis is organized in the following sequence:

- **Chapter 1:** Introduction to the research topic, including its significance and the main objectives of the study.
- **Chapter 2:** Literature review provides an overview of existing research on TDA and retaining walls and includes properties and behaviours of TDA, with appropriate case studies.
- **Chapter 3:** Development of a computational 2D finite element model of retaining wall backfilled with TDA. The model is validated by comparing its numerical results with the field test results.
- **Chapter 4:** Finite Element Model development of retaining wall at different backfill slope angles, by varying the width of TDA layer, to assess the earth pressure in each case and presents the results and discussions of the parametric study.

- **Chapter 5:** Conclusion summarises the key findings, significance of the study and provides recommendations for future works.

CHAPTER 2 LITERATURE REVIEW

2.1 Overview of Retaining wall

Retaining walls are constructed to sustain the lateral pressure of the earth behind them. They are structures used to contain soil or other loose materials when their natural steeps are undesirable, in the case when building linear infrastructures such as railways or roads. Retaining walls are often an overlooked critical asset of infrastructures because they are constantly around us. Each year, globally, millions of square meters of retaining walls are constructed for private and public projects. Retaining walls save space, reduce impacts, and allow owners to get the most out of a given property or right-of-way. Thus, retaining walls are an important part of development projects today (Medina et al., 2021).

In general terms, these structures may be classified into two groups, externally stabilized walls and internally stabilized walls. The examples of first category are gravity walls, reinforced concrete cantilever and reinforced concrete counterfort walls. These walls are essentially characterized by the concept that the lateral earth pressures due to self-weight of the retained fill and accompanied surcharge loads are carried by the structural wall. The construction sequence of these walls involves the casting of base and stem followed by backfilling with specified material. This requires a considerable amount of time as concrete must be adequately cured and sufficient time spacing must be allowed for concrete of previous lift to gain strength before the next lift is cast. The internally stabilized walls include metal strip walls, geotextile reinforced walls and anchored earth walls. These walls comprise of horizontally laid reinforcements which carry most or all

the lateral earth pressure via soil-reinforcement interaction or via passive resistance from the anchor block. This reduces the volume of concrete and steel reinforcement in the wall significantly, thus its construction is relatively fast speed. Retaining walls with relief shelves can be considered as a special type of retaining wall (Zastrow et al., 2017; Khan and Sikder, 2016; Shehata, 2016).

(Diwalkar, 2020) classified retaining structures based on attaining stability as follows:

- Gravity Walls: Gravity walls are stabilized because of their mass. They are constructed of dense, heavy materials like concrete and stone masonry, and they are generally reinforced structures. Some of gravity walls uses mortar, depending only on their weight to remain in place, as in the case of dry-stone walls. They are economical for only small heights.

- Semi Gravity Retaining Walls: In cross section these walls are usually trapezoidal. This type of wall is constructed in concrete and weight generates its stability. To reduce its weight, a small amount of reinforcement is provided. There are two sub types, cantilever retaining wall and counter fort retaining wall. Cantilever retaining wall uses action of cantilever to support backfill. This type of wall is most suitable up to 4m to 7m heights. Generally, these walls are of L and inverted T shape in cross section. For stability, they are constructed on solid foundations whose base is fixed to the vertical part of the wall and reinforcement is provided in the cantilevered base.

- Flexible walls: They are further classified into two types, sheet pile walls and diaphragm walls. Sheet piles are generally made of steel or timber. The timber

piles are usually limited to temporary structures whose driving depth is limited to 3m. steel piles are used for permanent structures and for depth of driving more than 3m. Diaphragm walls are mostly used for support systems in congested areas. They can be provided to support already existing structures. In this case there is no requirement of dewatering in construction. Diaphragm walls can be utilized for deep groundwater barriers through and under dams.

- Special type of retaining walls: These are Gabion walls and crib walls. Gabion walls are made by stacking and tying wire cages filled with trap rock or native stone on top of one another. They can have a continuous batter or be stepped back with each successively higher course. Crib walls are prepared with various materials including wood, concrete and even plastic. The cribs are made of interlocking headers and stretchers that are stacked like the walls of a log cabin. Crib walls are generally enough big.

2.2 Structural elements of Retaining Wall

Retaining walls are structures designed to resist the lateral pressure of soil or other materials. The structural element of retaining wall plays a crucial role in ensuring the stability, safety and performance of these structures. Figure 2.1 represents various components of a retaining wall. The following terms summarize the various structural elements of retaining wall, highlighting their function and importance.

- Wall Face: It is the exterior surface of retaining wall, directly exposed to the soil or backfill material.

- Wall Stem: It is the vertical component of retaining wall, which connects the wall face to the footing, and transfers lateral soil pressure to the footing and provides structural support and stability to the wall (Fan et al., 2019).

- Footing: The footing is the bottom most element of retaining wall, and it is responsible for transmitting the weight of wall and soil pressure to the underlying soil or foundation (Das et al., 2019). Its design and size are critical in ensuring the stability and safety of the retaining wall.

- Base Slab: It is a horizontal slab located at the base of the retaining wall, and it distributes the weight and pressure of the wall and soil evenly. It prevents settlement and ensures stability of the wall (Anand and Kumar, 2018).

- Counterfort: They are transverse walls built into retaining wall in order to provide additional stability and support (Olesiak and Wisniewska, 2018). They resist lateral soil pressure and reduce the risk of wall failure and enhance the overall structural integrity of the retaining wall.

- Weep Holes: They are small openings in the wall face, which allows water to drain from the soil and reduce hydrostatic pressure. They prevent water buildup, erosion and damage of the wall (Sivapriya et al., 2020)

- Drainage System: It is a network of pipes or channels designed to manage water flow and reduce pressure in retaining wall (Wang et al., 2022).

- Reinforcement: Materials such as steel bars or fibers are incorporated into the retaining wall to enhance its tensile strength, durability and resistance to cracking.

They improve the wall's structural integrity, ensuring its performance, safety and economic efficiency under various loading conditions (Kong et al., 2021).

- Capping: It is the top-most element of retaining wall and it protects the wall from weathering, erosion, and damage. It provides a finished surface, prevents water ingress and enhances the durability of the wall.
- Toe: It is the bottom-most edge of the retaining wall. Its design and construction are critical in ensuring the stability and safety of the wall.
- Heel: It is the portion of footing at the backfill side, it resists lateral pressure and ensures the wall's stability (Jasim and Yaqoobi, 2016).

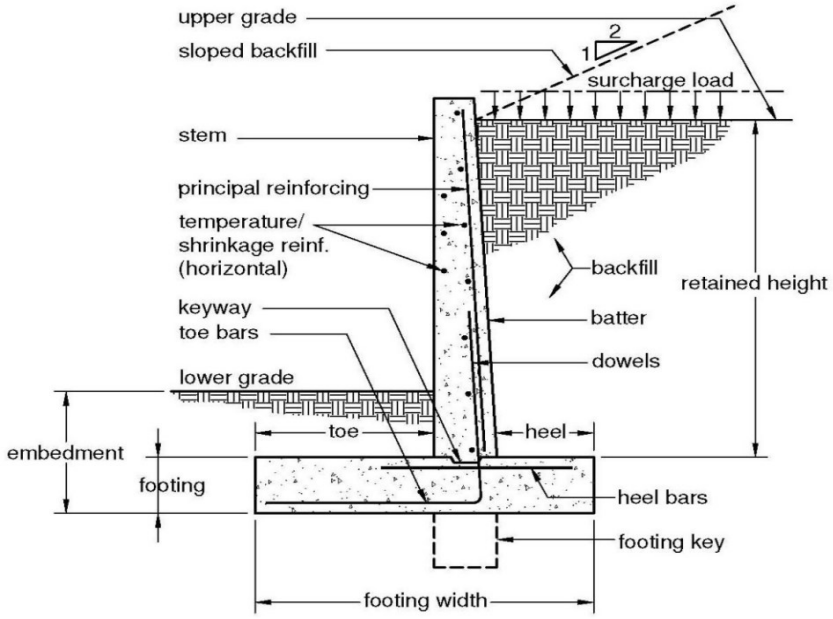

Fig 2.1 Visualization of terminology related to retaining wall (Hugh Brooks, Basics of retaining wall design, 10th edition)

2.2.1 Design considerations

- **Soil Properties**

The optimum design of reinforced concrete retaining wall is among the common optimization problems in civil engineering as it is affected by many different failure modes and input parameters. The properties of the foundation soil are one of the most critical input parameters in the optimum design of the retaining wall, just as in other civil engineering structures. While the existing foundation soil conditions on the site may sometimes be sufficient for an optimum design or it is necessary to consider alternative solutions such as ground improvement or foundation type change. Dagdeviren and Kaymak (2023) conducted a study to determine the effect of shear strength parameters of the foundation soil on the optimum wall cost using the modified artificial bee colony algorithm. In this study, optimum designs were performed separately for a total of 9246 different shear strength parameter combinations for a wide range, where the cohesion parameter was also considered in addition to the internal friction angle. The investigation results showed that, the shear strength parameters of the foundation soil are highly influential in wall costs under weak soil conditions but not under strong soil conditions.

In 2015 Gandomi et al., conducted a study on the effect of foundation soil properties on the cost of constructing retaining walls that are not too high. In his study, he considered retaining walls in between heights of 3 to 4.5 m, where there is no cohesion, and the internal friction angle is in the range between 28 to 38 degrees. Like any other engineering structure, the pressure under the foundation of retaining wall must be safely transferred to the foundation soil. The foundation type and dimension are clearly affected by the

properties of the foundation soil. The result of the study showed that as the internal friction angle increases from 28° to 38°, the wall cost decreases by about 17% on average.

In 2019, Uray et al., in his study on preliminary design guidelines for different wall heights and backfill internal friction angles, assumed that the properties of the backfill and foundation soil are the same. They chose the friction angle between the foundation and soil as $\delta = \frac{2}{3}\phi_{fill}$, and the foundation soil cohesion as c_{base}=0. It was observed that if the internal friction angle of foundation soil is less than 26°, in other words, δ<17.3∘, a feasible solution or an economical design is not possible. Therefore, ground improvement or wall type change is needed for optimal design in weak soil conditions. Therefore, in the construction of retaining wall soil properties plays a crucial role.

- **Loading Conditions**

Retaining walls are subjected to various loading conditions, including earth pressure, surcharge, seismic loads and wind loads. Shrawankar (2024) conducted a study to optimize the design of retaining wall using the software ANSYS. He used software tool such as AutoCAD to develop the model of the retaining wall. The geometry, dimensions, and structural components of the retaining wall were accurately represented. This included incorporating any variations in terrain, wall geometry, and material specifications. Following the CAD modeling phase, he generated a mesh. Meshing involves dividing the three-dimensional model into a finite number of elements, facilitating the numerical solution of equations governing the behavior of the retaining wall. External forces such as soil pressure, surcharge loads, and water pressure were applied, considering the specific conditions the retaining wall will encounter in its

intended environment. Finite Element Analysis (FEA) were employed to calculate displacements and stresses within the retaining wall structure. The shear stress induced on a retaining wall is a critical factor in assessing its structural stability and performance. Shear forces are developed along the interface between the retaining wall and the backfill soil, primarily due to lateral earth pressure. Understanding and analyzing the distribution of shear stress is essential for evaluating potential failure modes, such as sliding and overturning. The research has systematically explored and presented a comprehensive investigation into the design and analysis of retaining walls under various loading conditions.

National Concrete Masonry Association (2010) states that, vertical surcharge loadings are imposed behind the top of the wall in addition to load due to the retained earth. These surcharges add to the lateral pressure on the retaining wall structure and are classified as dead or live load surcharges. Live load surcharges are transient loadings. They may change in magnitude and may not be continuously present over the service life of the structure. In this design methodology, live load surcharges are considered to contribute to destabilizing forces only, and they are considered to have no contribution to stabilizing the structure against external or internal failure modes. Examples of live load surcharges are vehicular traffic and bulk material storage facilities. Whereas dead load surcharges are considered to contribute to both destabilizing and stabilizing forces since they are usually of constant magnitude and are present throughout the life of the structure. The weight of a building or another retaining wall are examples of dead load surcharges.

- **Drainage**

Drainage and water management are critical aspects of retaining wall design. In 2017 Boeckmann et al., constructed two model retaining walls measuring 8 ft wide by 4 ft tall in the large-scale geotechnical modeling laboratory at the University of Missouri. The first wall retained silty sand backfill, and the second wall retained fine sand backfill. For each wall, the researchers performed a series of tests to evaluate performance of drainage features installed in the wall face. The drainage features varied in type (conventional weep holes and maintainable drains), size (diameters of 2, 4, and 6 in.), and spacing along the wall face. To test drain performance, a constant height of water was impounded behind the wall backfill while measuring outflow from the drains and pore pressures within the backfills. The results from the study indicated that, drain outflows from the fine sand model were one to two orders of magnitude greater than drain outflows from the silty sand model and indicates that both drain outflow and drawdown within the backfill increases with drain size. Both weep and maintainable drains were tested in the fine sand model. The effect of drain type depended on drain size. For 2 in. diameter drains installed at the same effective spacing, the outflow and drawdown values were similar regardless of drain type. For 6 in. diameter drains, the outflow and drawdown were approximately twice as great for the maintainable drain as for the conventional weep hole. A likely explanation for the difference between drain types is that the conical maintainable drains have a greater surface area compared to planar weep holes, which promotes increased drainage. The surface area effect is muted for smaller diameter drains, not only because the difference in surface area is less, but also because most of the increased surface area is contained in the wall face opening as opposed to being in contact with the backfill soil.

- **Stability**

In 2017 Karkanaki et al., conducted a study based on a new algorithm for design of cantilever retaining walls based on the proposed failure mechanisms and considers the effects of wall geometric parameters using an upper-bound limit analysis approach. In this study, the upper-bound limit analysis method was used to determine the shape of the critical failure mechanisms for a retaining wall simultaneously with its optimal dimensions. The safety factors against overturning, sliding, and bearing capacity failure were assessed by the limit analysis approach. A retaining wall of 6m height was modeled in PLAXIS 2D software and analysed. Results were drawn for total displacement sliding stability failure and total displacement deep shear failure. The safety factor was also calculated through a conventional approach for the design of cantilever retaining walls. Comparing the results of this study with the findings of other researchers suggest that the failure mechanism proposed for determination of active pressure, stability, and safety factors of the retaining wall produce simple yet accurate results and that the results obtained with the proposed failure wedges are entirely consistent with the results from the finite element method. The results show that the geometric dimensions of the wall affect its safety factors and the active pressure on the wall. Consequently, for determination of the most critical state of failure (the lowest safety factors and the highest active pressure), the failure wedges should be optimized while simultaneously determining the optimal wall geometry that can induce the critical state of soil failure. The results show that the length of the heel at the base of the wall affects the magnitude and direction of the active pressure on the retaining wall. The goal of calculating this pressure is not to just determine the maximum force but to use it for stability checks against overturning and to evaluate

the structural strength. Therefore, when determining the critical condition of the wall, the designer should optimize both the magnitude and the direction of the force acting on the wall.

In 2021 Mazni et al., reported that the failure of retaining walls is mainly caused by the incorrect design of retention and support systems. In the laboratory he made retaining wall blocks with mixture of cement, sand, and water and dimension 9.9 (length) x 5 cm (width) x 5 cm (height). The blocks were arranged in a glass box with a dimension of 40 cm (length), 10 cm (width), 80 cm (height). The surface of the embankment behind the wall was in level, with the soil type being sand. The total height of the wall was 40 cm, and there were 11 blocks in total. There was no connection between the concrete blocks. The static load was given gradually until the wall fails. An equation function was determined to study the failure pattern. This equation's function helped to determine the wall's overall stability, as well as the backfill area and length. Analysis for overall stability using the slices method applies to flat, circular, or a combination of both. With the method of slices, the soil block that has failed was divided into several slices. Vertical slicing was used to divide the slices. For each piece, the working forces were analyzed and calculated cumulatively. Furthermore, the safety factor of the assumed failure plane was calculated by comparing the resisting and driving forces. It is necessary to re-design the block retaining wall dimensions to obtain a safe overall, sliding, and overturning stability value.

- **Sustainability and Environmental Impact**

Sustainability and sustainable development relate to the capacity to carry out construction with minimal economic, societal and environmental impact. In the past, the final selected

solution was typically based on a compromise between minimum costs and maximum functionality. Today, an appropriate sustainability analysis approach is often recommended so that environmental and social impacts are part of the solution decision process. From a total sustainability point of view there are three pillars or requirements: environmental, economic and societal that can be assessed from "cradle to grave" (Josa and Alavedra, 2006).

In 2020, Damians et al., conducted a study to select the best sustainable option from conventional gravity wall, cantilever wall types, steel and polymeric soil reinforced mechanically stabilized earth (MSE) walls of 5 m height. Analyses were carried out using the MIVES methodology which is based on value theory and multi-attribute assumptions. Using this methodology indicator issues were scored, weighted and aggregated to generate final numerical scores that allow solution options to be ranked. The final scores include an adjustment based on stakeholder preferences for the relative importance of the three sustainability pillars (environmental, economic and societal/functional). The analysis results show that MSE wall solutions are most often the best option in each category compared to conventional gravity and cantilever wall solutions and thus most often the final choice when scores from each pillar were aggregated to a final score.

2.2.2 Design Codes

Retaining walls support the lateral thrusts produced by the retained material. To fulfill this purpose, these walls use their weight and the weight of the material placed on their foundation to stabilize themselves. The designs of retaining walls must meet requirements

of functionality, safety, strength, and economy that depend on the regulations of each country (Diaz et al., 2021). An overview of retaining wall design building codes and standards from major regions including North America, Europe and Asia is given here highlighting the key requirements, design considerations and construction practices.

- **North America**

    - **IBC Guidelines (International Building Code)**

Designing retaining walls in accordance with American standards is critical for ensuring compliance, safety, and structural integrity. The International Building Code (IBC) is the principal source of construction and design standards in the United States. The IBC establishes criteria for structural design, materials, and building techniques, including those applicable to retaining walls.

The IBC requires retaining walls to be designed to resist overturning, sliding, excessive foundation-bearing pressure, and water uplift. Retaining walls shall be designed to resist lateral soil loads. Soil loads specified in IBC shall be used as the minimum design lateral loads unless determined otherwise by a geotechnical investigation. Retaining walls in which horizontal movement is restricted at top shall be designed for at-rest pressure. Whereas, retaining walls free to move and rotate at the top shall be permitted to be designed for active pressure. The design of walls retaining more than 6 feet of soil and located within Seismic Design Category D or above are also required to be checked for seismic earth pressure. The design is required to meet a minimum safety factor of 1.5 in relation to sliding and overturning. If the design includes the seismic earth pressure, the

safety factor for sliding and overturning can be reduced to 1.1 (International Building Code, 2018).

- **ACI Standards (American Concrete Institute)**

The American Concrete Institute (ACI) provides standards for design and construction of retaining wall by ensuring safety and durability. The reinforced concrete stem and footing flexure and shear design strengths must be at least equal to the factored moments and shears determined from the wall analysis using the forces and reactions. ACI standards require resistance reduction factors to be applied for various resistances, including 0.9 for flexure resistance and 0.75 for shear resistance, load factors to be applied for various loads like a factor of 1.6 for lateral earth pressure and a factor of 1.2 for self weight of the structure. According to ACI guidelines factor of safety against sliding failure is set to be greater than or equal to 1.5, factor of safety against overturning failure is set to be greater than or equal to 2 and factor of safety against bearing failure is set to be greater than or equal to 3 (ACI 318-19).

Wall stem - According to ACI code, retaining wall stems are designed as one-way slabs in accordance with the applicable provisions of the code. Design of the stem is typically done by considering a unit length of wall as is done for one-way slab design. The wall thickness is sometimes tapered to provide material savings as the moment and shear demand decrease nearer the top of the cantilever. A tapered front face, however, complicates the formwork construction and reinforcement layout. Consequently, often the wall thickness is kept constant on stems of lower height. The minimum recommended stem thickness is 8 in., but many engineers prefer minimum 10 in. Code indicates that for

walls of uniform thickness, the critical section for flexure and shear should be taken at the interface between the stem and footing. For walls with varying thickness, shear and moment should be investigated throughout the height of the stem. Axial loads, including the wall stem weight and frictional forces of the backfill acting on the wall stem, should be considered in the stem design in addition to bending due to eccentric vertical loads, surcharge loads, and lateral earth pressure (ACI 318-19).

Buttresses and counterforts - According to Code, the stem of a counterfort or buttressed cantilever retaining wall should be designed as a two-way slab using the applicable provisions of code. Buttresses or counterforts are analyzed and designed as rectangular beams. Horizontal reinforcement connects the stem to buttresses or counterforts, and vertical reinforcement connects the footing to the buttresses or counterforts (ACI 318-19).

Wall footings—According to ACI standards, wall footings for cantilever retaining walls should be designed as one-way shallow foundations using the applicable provisions of the code (ACI 318-19).

- **Europe**

    - **Eurocodes (European Standardisation System relating to construction)**

Eurocode is a set of European standards for structural design, developed by European Committee for Standardization (CEN). Eurocode 7 (EC7) provides guidelines for design and construction of retaining wall. Eurocode 7 is based on the limit state design method, with the design principles and requirements for the safety, serviceability and durability of structures set out in the head Eurocode, EN 1990 (CEN, 2002). Eurocode 7 also refers to

the many new European normative standards (ENs) for geotechnical investigations and testing, and for the execution of geotechnical structures. Hence Eurocode 7 differs from the former British Standards (BSs) published by the British Standards Institution (BSI) for geotechnical design in its nature, in its use of the limit state design method and through its reference to ENs for geotechnical investigation, testing and execution, which have requirements and specifications that differ from those in the former BSs (Orr, 2012).

According to EC7, retaining walls shall be designed to resist soil and water pressure. A soil investigation shall be performed to determine soil properties and behavior. These investigations shall include laboratory testing and field observations and then selecting characteristic values of soil parameters for use in design before carrying out any design calculations (Orr, 2012).

The limit state design method in Eurocode 7 normally requires that separate calculations be carried out to check that the occurrence of an ultimate limit state (ULS) and a serviceability limit state (SLS) are sufficiently unlikely. A consequence of this is that designs to Eurocode 7 require that more attention than heretofore be given to the prediction of foundation settlements and ground movements. Hence there is a need for reliable geotechnical investigations and testing methods to determine soil stiffness and compressibility parameters, and for improved methods to calculate deformations (Orr, 2012).

EC7 introduced three design approaches (DAs), to take account of the special features of soil, and to accommodate the different design traditions and views in Europe on how partial factors should be applied in geotechnical design. Design approach 1 with partial

factors applied in separate combinations either to just the actions or to the material properties and the variable actions. Design approach 2 with partial factors applied to the resistances and to the actions or action effects. Design approach 3 with partial factors applied to both the actions and the material properties. The introduction of three Design Approaches has enabled the use of either partial material factors or partial resistance factors, and hence has accommodated different national design practices and preferences in Europe (Orr, 2012).

- **Asia**

    - **India - Bureau of Indian Standards (BIS Code)**

The Bureau of Indian Standards (BIS) provides guidelines for selecting the type of retaining wall suitable for each site, considering factors like soil type, slope stability and seismic activity. According to IS 4458, the allowable bearing capacity shall be calculated in accordance with IS 6403 based on soil test data. In case of non-erodible rocks, the bearing capacity shall not exceed one-half the unconfined compression strength of the rock if the joints are tight. Where the joints are open, the bearing capacity shall not exceed one-tenth the unconfined compression strength of the rock. The value of cohesion (c) and angle of internal friction (ϕ) vary for different backfill and foundation materials. These values shall be determined by experiment (IS 4458, 1997).

The design of a retaining structure shall as per IS 4458 consist of two principal parts, the evaluation of loads and pressures that may act on the structure and the design of the

structure to withstand these loads and pressures. Self weight of the retaining structure, live load and imposed loads, earth pressure acting on the wall, water pressure due to water table or subsurface seepage, water pressure due to water table on toe side, seismic forces and special loads if any are the forces that shall be accounted for the design of retaining wall. Retaining walls and breast walls shall be designed as rigid walls, using following criteria:

- Factor of safety against overturning should be greater than 2 for static loads and greater than 1.5 for earthquake loads.
- Factor of safety against sliding should be greater than 1.5 for static loads and greater than 1 for earthquake loads.
- Maximum base pressure should be less than or equal to q_a (Allowable bearing capacity) and should be less than or equal to $1.33q_a$ for earthquake loads.
- Minimum base pressure should be greater than zero.
- Factor of safety against floatation should be greater than 1.25.

The depth of retaining wall and breast wall below ground level or terrace level shall be at least 500 mm below side drain within soil or highly jointed rock and foundation shall be on natural firm ground. In case of steep slopes ($>35^0$), retaining walls with front face nearly vertical and back-face inclined shall be used as it will reduce the height of wall considerably. A dip of the base of wall towards hillside to the extent of 3: 1 (horizontal: vertical) proves very economical in seismic conditions. It increases factor of safety against

sliding significantly. As part of drainage plan, inverted filter shall be provided behind retaining walls to drain off ground water table or rainwater seepage. In addition, weep holes shall be provided in cement stone masonry walls at spacing of about 1.5 m centre-to-centre in neither direction. The size of weep holes shall be 100 mm to 150 mm PVC (flexible) pipes and shall be embedded at 10^0 down from the horizontal towards valley side to effectively drain the water from ground (IS 4458, 1997).

2.3 Analysis of Retaining Wall

Retaining walls are designed to resist lateral earth pressure and withstand seismic forces generated by potential earthquakes in the area. Coulomb and Rankine provided the first scientific applications to design of retaining wall by defining the solution of the lateral static earth pressure problem.

In 2015, Vijayakumar et al., conducted a study on semi- gravity retaining wall to check its stability in Dewarwadi hamlet in Karnataka, India. Figure 2.2 shows the image of this existing retaining wall. Analysis was carried out in a retaining wall with length 25.5m, top width 0.55 m, height 3.98 m, base slab width 2.65 m, and foundation depth 1.46 m. There were 6 weep holes with a diameter of 100 mm and 26 holes with a diameter of 50 mm. The safety factors for bearing failure, skidding, and overturning were established. Additionally, because the existing wall is of the semi-gravity type, Rankine's theory was used to calculate passive resistance in the foundation soil and Coulomb's theory was used to calculate active earth pressure due to backfill. The current retaining wall was found to be secure since it exceeds the necessary factors of safety for overturning, sliding, and

bearing failure values of 1.5-2, 1.5-2, and 3, respectively. Additionally, the average factors of safety for overturning, sliding, and bearing failure were found to be 4.56, 9.62, and 3.10, respectively. The wall was therefore found to be big and ineffective. As per the analysis, new dimensions were proposed for the retaining wall with stem top width of 0.2 m, stem bottom width of 1.1 m, base slab width of 2.72 m, base slab thickness of 0.68 m, heel projection of 0.62 m, and toe projection of 1 m. Overturning, sliding, and bearing failure each were found to have safety factors of 3.684, 6.970, and 5.140, respectively. When compared to the current wall, the proposed wall was found to use 41.5% fewer materials.

Fig 2.2 Existing Retaining wall at Dewarwadi (Vijayakumar et al., 2015)

In 2018, Dhamdhere et al., carried out a comparative study between cantilever and relieving platform retaining wall with different heights from 3 to 10 meters and an SBC of 160 KN/m^2. Comparative analyses of cost, bending moment, and stability against overturning and sliding between the two retaining walls were studied. The relieving platform was located at the midpoint of the retaining wall, and the following design parameters were used, length of relieving platform was kept equal to the length of heel

slab, thickness of relieving platform was one-fourth of base slab thickness, angle of friction was 35^0, coefficient of active earth pressure (Ka) was 0.27 and coefficient of passive earth pressure (Kp) was 3.6. The soil's bearing capacity ranged from 100 KN/m^3 to 200 KN/m^3 at intervals of 10 KN/m. Soil of weight 18KN/m^3 and concrete of weight 25 KN/m^3 was used. The retaining wall design incorporated stability evaluations like, the factor of safety against sliding was decided to be larger than 1.5, and the factor of safety against overturning was chosen to be greater than 0 and less than the soil bearing capacity. The eccentricity of the resulting reaction force was determined to be between 0 and the base width of 6. The IS456:2000 code was used to calculate the reinforcement spacing as well as the highest and lowest reinforcement percentages. From his study he concluded that the relieving platform retaining wall, was less expensive and more stable than the cantilever retaining wall and does not have the heel component's bending moment.

Chowdhury et al., in 2013 evaluated the performance of gravity type of retaining wall for earthquake loading. In his study, he considered the backfill soil of the retaining wall to be dry and cohesionless. Backfill soil was taken to be sandy, and ground was considered to have no slope. They proposed mathematical model for the same case. Their model assumes that the active pressure is mobilized already so it cannot induce any stiffness to overall dynamic response and there will be inertial effect. Also, as thickness of wall is sufficient, they considered stiffness contribution, thus wall was considered to contribute to stiffness and inertia. Wall was assumed to be fixed at base. They worked out dynamic flexural and shear response and used finite element method to perform response. At the vertical face of wall, backfilled soil mass was added as lumped mass. The pressure of backfilled soil was hydrostatic in nature. They used ANSYS software for the analysis.

In 2015, Sanjei et al., selected various retaining wall's shape by performing preliminary calculations. He conducted finite element analysis using PLAXIS. He considered two ways of construction first one was to carry out backfilling after the wall construction and other is to do backfilling parallel to wall construction. He generated finite element model for his analysis. He selected three different shapes with constant height and cross-sectional area. He estimated the exerted force on retaining wall first by using Coulomb's method of analysis and wedge method. He assumed few basic properties of soil and designed wall as mass concrete and calculated optimal base size for three walls. He then considered the stability check. According to him, in the use of PLAXIS software, one must consider appropriate size of geometry and boundary conditions. To determine the sequence effect of construction, he divided backfill soil into layers of 0. 5m thickness. Calculation for both phases worked out in his study.

2.4 Finite Element Analysis (FEA)

The construction industry has undergone significant transformation in recent years, driven by advances in technology and the need for more efficient and sustainable practices. One such technology that has gained widespread acceptance is Finite Element Analysis (FEA). FEA is a numerical method that uses algorithms and mathematical models to simulate the behavior of complex systems, including structures, under various loads and conditions.

Purkar and Kute (2015) conducted a finite element analysis on a rigid retaining wall using the software FORTRAN-77. The system was modeled as a plane strain two-dimensional

problem. The investigations were conducted to examine the influence of reinforcement, stiffness and poison's ratio of backfill and foundation strata on the performance of a rigid wall. A concrete wall of 200 mm thick and a concrete strip footing of width 1.5 and 0.45 m thick were considered in the analysis. The concrete wall and footing were assigned the values of the (E, m, γ) that of concrete of M25 grade. The 2D FEM analysis is carried out considering self weight and a surcharge load of 40 kPa, by the software used in the current study to determine the front face deformations. The results obtained were validated with those presented by Shridevi and Garg (1997). The comparison between the results showed that the lateral displacements calculated by using the software near the top edge of the wall is slightly higher than the values reported by Shridevi and Garg (1997). However, at other locations these results were in good agreement.

In 2018 Hulagabali et al., carried out a study to focus on the parametric sensitivity analysis of MSE walls using a numerical model, which uses the finite element method (FEM) to determine the factors of safety of the wall and its comparison with the analytical methods. The finite element computer program, GEO5 FEM was used to develop the numerical model and the GEO5 MSE was used for the analytical method. The MSE walls were analysed for horizontal and vertical movements with respect to length of the reinforcement. External stability analyses were also carried out for overturning, sliding and bearing capacity, for three different soil types. Geogrid reinforcements are checked for the factor of safety with respect to pullout resistance and tensile strength and against the height of the wall for three different backfill soils. The global factors of safety obtained from the FEM and AASHTO method for three different soils with different lengths of the reinforcement are compared with each other. From FEM and AASHTO methods, it was

observed that FEM gives little higher factor of safety than AASHTO method. This is because of discretization of single structure into number of nodes, element and regions. So, it gives more convenient results than other methods. Based on the comparison, it was noted that both the analyses have provided acceptable range of safety values and are in good agreement.

Saikia and Bhattacharjee (2021) presented a study on the response of the multi-tiered geosynthetic reinforced soil wall subjected to seismic excitation using PLAXIS 2D software. The modeled wall was 2.8 m high, 4 m long and 2 m wide and was constructed on a 20 cm thick soil foundation. The wall was backfilled with medium dense Tokachi port sand (Dr = 55%) and reinforced with PET geogrid. Geogrids were placed at vertical intervals of 60 cm. The foundation soil was given the same properties as the backfill soil but at a relative density of 90%. The wall and backfill soil were modeled using 15 nodded triangular elements. The results in terms of horizontal displacements, lateral and vertical stresses of the shake table test as reported by Ling et al., (2005) were compared with the results obtained from the finite element model. The compared results were reasonably in good agreement for displacements and lateral stresses. However, the vertical stress was found to be maximum near the facing wall where the literature value was found to be slightly high than computational value.

2.5 Tire Derived Aggregate (TDA)

Tire-derived aggregate (TDA) is a relatively new construction material and is produced by mechanically shredding scrap tires, typically measuring from 12 to 305 mm in size. It is commonly used in construction projects because it is sustainable, lightweight, and less expensive than many competing available materials (ASTM D6270-08). Figure 2.3 represents an image of scrap tires processed into tire derived aggregate (TDA).

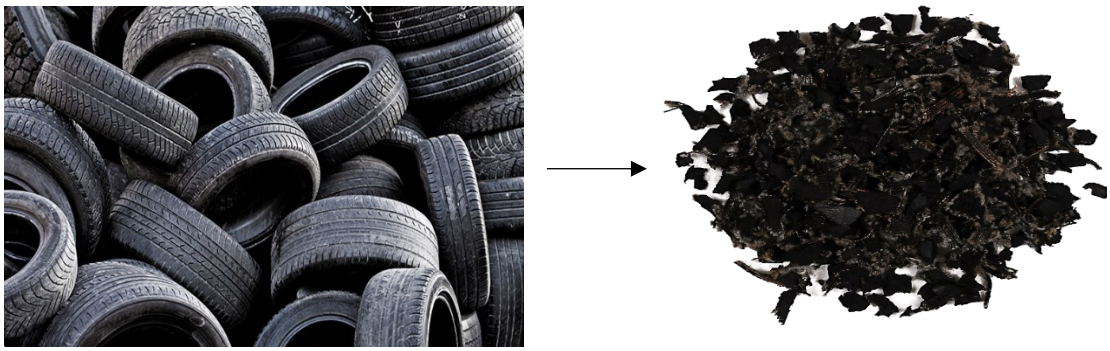

Fig 2.3 Scrap tires processed into TDA (Shutterstock, Inc.)

TDA is categorized into two size ranges in accordance with the specifications set forth in ASTM D6270-08. The specified size ranges are termed as Type A, suitable for drainage, vibration damping, and insulation applications, and Type B, suitable for use as a lightweight embankment fill, wall backfill, and some landfill drainage and gas collection applications. The primary benefit of TDA as a construction material is its low unit weight. The unit weight of compacted TDA is one-third to one-half that of typical compacted soil. (Ahn et al., 2014).

2.5.1 Properties of TDA

- **Gradation**

Type A TDA has a maximum dimension of 200mm measured in any direction. In addition, Type A TDA is required to have the following square mesh sieve passage rates, 100% passing in 100-mm sieve, a minimum of 95% passing (by weight) in 75mm sieve, a maximum of 50% passing (by weight) in 38mm sieve and a maximum of 5% passing (by weight) in 4.75-mm (ASTM D-6270-08).

Type B TDA has a minimum of 90% (by weight) with a maximum dimension, measured in any direction of 300 mm and 100% with a maximum dimension in any direction of 450 mm. In addition, Type B TDA is required to have the following square mesh sieve passage rates, a minimum of 75% passing in 200mm sieve, a maximum of 50% passing (by weight) in 75mm sieve, a maximum of 25% passing (by weight) in 38mm sieve, and a maximum of 1% passing (by weight) in 4.75-mm sieve (ASTM D-6270-08).

- **Unit Weight**

TDA has a low unit weight compared to typical soils, usually one third to one half of the unit weight. Typical unit weights of TDA range from 320 kg/m^3 (20 lb/ft^3) to 657 kg/m3 (41 lb/ft^3) depending on the size, content, and compaction technique.

- **Settlement Properties**

In 1992, Manion et al., designed a special apparatus to accommodate the high compressibility of TDA and to measure lateral stresses. From the test results the

coefficient of earth pressure at-rest (Ko), Poisson's ratio (μ), and young's modulus (E) was determined to be: Average Ko at less than 23 psi = 0.44, Poisson's ratio (μ) at less than 23 psi = 0.30 and Averaged secant at 10% strain young's modulus (E) = 18.1 psi.

Tweedie et al., in 1997 installed settlement plates in a retaining wall field testing facility to determine the compression and settlement characteristics of TDA for at-rest conditions. Material from three different suppliers was placed, compacted, and then subjected to four different surcharge loads. Laboratory tests were also performed by Humphrey et al., in 1992. A comparison of the vertical strain (%) found from field testing versus laboratory testing was conducted. The vertical strain predicted from lab testing was greater than measured in the field due to self-compression of the TDA beneath the plate prior to the initial reading thereby moving the average state of stress to a flatter portion of the compression curve (Labbe, 2018).

2.5.2 Overview of TDA

- **Advantages of TDA**

Recycling scrap tyres can be challenging due to their large size, but it is worth the additional effort. The primary benefits associated with rubber recycling include a lower consumption of energy, less pressure on natural rubber, the conservation of landfill space,

a reduction in environmental pollution, and the creation of new products (Farooq et al., 2022)

- Conservation of landfill space: Tyres occupy ample space in landfills. Landfill space is limited and expensive. Hence, using scrap types helps save this space for things which are difficult to recycle (Cerminara et al., 2018).

- Creation of beneficial products: Recycled tyres can be converted into various valuable products like tyre-derived fuel, rubberised asphalt, flooring material, railway sleepers and playground turf (Farooq et al., 2022).

- Prevention of the spread of diseases: Discarded scrap tyres serve as a habitat for the growth of disease-carrying rodents. Moreover, stagnant water gets collected inside them, which serves as a breeding ground for flies (Farooq et al., 2022).

- Prevention of fires and pollution: One of the significant disadvantages associated with stockpiling scrap tyres is fire hazard. For example, a fire broke out in Melbourne in 2016, and more than 150,000 tyres were burnt, which led to the release of harmful gases into the environment. Hence, re-using these scrap tyres is highly recommended and stockpiling should be avoided.

- Economic benefit: TDA costs less than conventional civil engineering materials while, at the same time, its comparative lightness reduces transportation costs. A cost-benefit assessment was performed for CalRecycle to evaluate projects where TDA was used in place of conventional soil fill materials. Findings showed that the material and transportation costs of TDA are much cheaper than all other studied materials that included crushed gravel, floating concrete slabs, pumice

rock, expanded polystyrene, expanded shale clay, and wood chips. For example, in Sonoma County in California, where a mountain road has washed away every ten years, TDA helped bring the cost of repairs in at 50% of the county's estimate (Cheng, 2016). Figure 2.4 represents the life cycle and various civil engineering applications of scrap tyres.

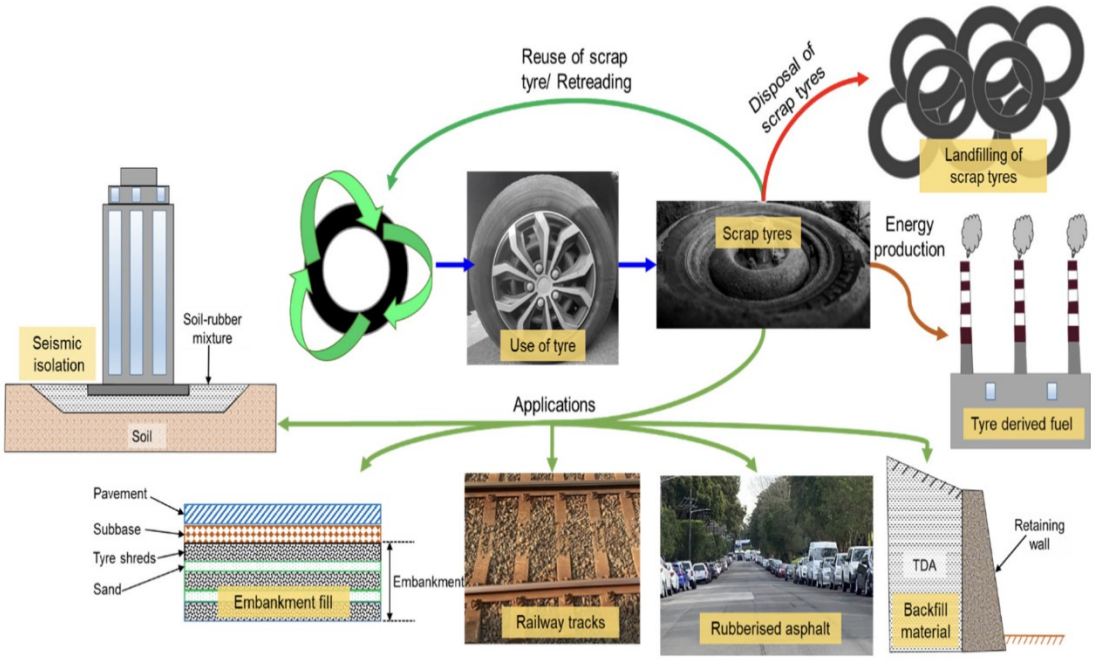

Fig 2.4 Life cycle and civil engineering applications of scrap tyres (Farooq et al., 2022)

- **Limitations of TDA**

It has been found that in numerous civil engineering applications, TDA encounters water, which may lead to the leaching of organic and inorganic compounds, potentially compromising the quality of surrounding ground and surface waters.

Park et al., in 2023 conducted a study to examine TDA's physical, chemical, and microbiological properties, along with a study on the leaching of tire components and their ecological and human health issues. It has been noted that although end-of-life tires leach tire components, tires can also adsorb potentially toxic synthetic organic chemicals (SOCs) from the water. Metals leached from TDA, or tire chips were found to be below the detection limit or did not exceed federal and state Maximum Contaminant Levels (MCLs) under field conditions at a pH between 6.5 and 8.5. Iron and zinc were the dominant metals leached from TDA.

Although leached compounds from tire-wear particles and particles themselves have been found to be toxic to a few specific aquatic species, no conclusive study has shown the harmful effect of TDA on aquatic species. The low concentration of leached substances and the dilution effect suggest that using TDA in civil engineering projects is unlikely to cause significant toxicity to aquatic species and humans. Consequently, it can be asserted that the potential health risks associated with exposure to leached chemicals from TDA in civil engineering projects are minimal.

- **Applications of TDA in Construction Industry**

Mahgoub and El Naggar (2019) conducted a study on the design of shallow foundations built on TDA layer. Shallow foundations are comparatively cheaper to construct as it does not require any special construction equipment. Major issues concerning structures built on soft soil are they face serious safety issues like settlement, stability and inadequate surface bearing capacity which in turn leads to sliding failures and structural damage which results in social and economic loss. In this study, they constructed three rigid concrete square footings to examine the behaviour of shallow foundations built on a backfill of TDA materials. For the first footing, the soil beneath the footing was replaced by compacted granular backfill of 1m. The second footing was casted on 0.5m of granular backfill which overlayed on a TDA layer of 0.5m and the third footing was casted on 0.3m granular backfill which overlayed on 0.7m TDA layer. To investigate the performance of each configuration, field tests were designed to measure the loads applied to the concrete footings, the corresponding footing settlement, and the stresses beneath the TDA layer. A 240mm pressure cell was installed under the backfill to measure the stress transfer through the backfill. Footing settlement was monitored by using four linear variable differential transformers (LVDT). The load was applied using a hydraulic jack that was installed at the centre of the top surface of the concrete footing. A maximum load of 340 KN was applied to the first footing and 260 KN for the second and third footing. Loading was stopped when the truck was lifted due to the force applied by the hydraulic jack in the first footing, or when a clear punching shear failure could be seen in second and third footing. They also developed a computational model using PLAXIS 3D to validate the results of

the numerical analysis. From the results, they concluded that in comparison to the use of conventional backfill, the use of a TDA layer underneath shallow foundations achieved a significant improvement in transferring the stresses and reducing the stress influence zone beneath the footing.

In 2022 Farooq et al., presented a study on the applications of TDA in railway projects. In this study, they developed finite element model for ballasted track and slab track using ABAQUS software. The parts were modelled using eight-noded hexahedral linear brick elements with reduced integration. The total elements in the ballasted and slab tracks were 15262 and 15116, respectively. Both track models were restricted from displacements in the x, y, and z directions and a pinned support boundary was applied to the base of the models. A TDA layer of thickness 25 mm was used for the simulations, and TDA was placed below the sub ballast and base layers of ballasted and slab tracks, respectively. The stress transfer in ballasted and slab tracks with depth was analysed for different train speeds and axle loads. To study the effect of train speed and axle load, only one parameter among train speed or axle load, was varied, whereas the other was kept constant. From the analysis he concluded that, there is an increase in shear stress for ballasted track with TDA layer while there is a reduction in shear stress in slab track when TDA layer was incorporated on the sleeper top, whereas shear stress at lower layers of the ballasted track, that is, subgrade top and bottom, reduces by 96.5% and 87.5%, respectively, on TDA incorporation and there is a maximum reduction in shear stress for the lower layers of a slab track of around 67% and 46% at subgrade top and bottom respectively, after TDA incorporation. The shear stress results show that the addition of TDA helps to reduce the shear stress on the concrete slab of slab track, while shear stresses are increased for a

ballasted track after TDA incorporation. However, TDA effectively reduces shear stresses for the lower layer of both track types.

Arulrajah et al., (2019) in his research conducted an evaluation to determine the engineering properties of recycled concrete aggregates (RCA) blended with tire derived aggregates (TDA). The RCA-TDA blends were evaluated to assess their geotechnical suitability for construction of pavement subbases. He collected RCA with nominal size of 20mm from a demolition recycling site in Victoria, Australia and 3 different sizes of TDA aggregates were collected from a tire recycling company in Victoria. The small size TDA ranged from 1 mm to 3 mm, the medium size aggregates ranged from 2 mm to 4 mm and the large size aggregates ranged from 8 mm to 15 mm. The samples collected from the recycling sites were oven dried and subsequently mixed thoroughly to minimize segregation and changes among the samples. TDAs were added in proportions of 1%, 2% and 3% by weight to RCAs, mixed and quartered into subsamples for performing the laboratory tests. The geotechnical laboratory tests undertaken included particle-size distribution, pH, plasticity index, organic content, Los Angles abrasion, particle density, water absorption, flakiness index, modified compaction, California bearing ratio (CBR), permeability, permanent deformation and Repeated Load Triaxial (RLT) tests. The results of the laboratory testing undertaken in this research have shown overall that the incorporation of TDA into RCA had low to minimal effect on the physical and mechanical properties of the original RCA such as pH value, LA abrasion and permeability. The CBR value of the RCA was decreasing by increasing the percentages of the TDA. The grading limits of all RCA blends were found to be within the local road authority specified limit for subbase materials. However, the CBR value for all blends still met the minimum

requirements of local authority to be used as subgrade material. The research indicated that using TDA with RCA lowers rigidity and cracking, thus resulting in a longer pavement service life. Three available TDA was evaluated in this research in blends with RCA to be used as subgrade materials. The mechanical properties and geotechnical characteristics of the RCA-TDA blends indicated that addition with up to 3% TDA by weight generated viable geomaterials for pavement subbase applications.

2.5.3 Effect of TDA on stability and performance of Retaining wall

For the past two decades, TDA has been used in various civil engineering applications including subgrade and embankment fill, retaining wall and bridge abutment backfill, subgrade insulation to limit frost penetration, and lateral edge drains. Tweedie et al., (1997) constructed a full-scale test facility at the University of Maine to test the effects of TDA placement behind a retaining structure. The testing facility was designed to accommodate approximately 100 m^3 of backfill. It measured 4.88 m x 4.47 m x 4.57 m in plan. The foundation and sidewalls consisted of reinforced concrete. The back wall of the facility consisted of removable timber lagging, allowing backfill to be removed after the completion of a test. An overhead crane was installed to hoist backfill and surcharge into the facility. The front wall of the facility was designed as the retaining wall. It consisted of three reinforced concrete panels with the instrumentation placed on the center panel to reduce the influence of friction on the side walls. TDA was placed in 200 mm lifts and compacted with a vibratory tamping foot roller with a 1180 kg static weight. For all tests, the surface of the backfill was horizontal. TDA from three different manufacturers was

tested. After TDA placement, as surcharge of 35.9 kPa was applied. Measurements were taken during the at-rest state and at wall rotations ranging from 0.01H to 0.04H, where H is the wall height. After rotation, the time dependent change in horizontal stress was investigated for some trials. The horizontal stress distributions for all three samples proved to be very similar. Before rotation of the wall (at-rest conditions) stress decreased slightly with depth but as the wall was rotated to 0.01H the horizontal stress decreased significantly at the top but decreased only slightly at the bottom of the wall. The horizontal stress distributions for all three samples during active conditions were very similar as well. As the wall was rotated outward the horizontal stress decreased significantly at the top of the wall, however the decrease in horizontal stress at the bottom of the wall was small. The magnitude of the resultant horizontal force increased when time was allowed to pass after rotation of the wall, with a 20% increase one day after initial rotation.

Ahn and Cheng (2014) presented a study to evaluate the dynamic performance of TDA backfill in RW under simulated earthquake loads based on a full-scale shake table test. The retaining wall in the test was a semi-gravity reinforced concrete cantilever wall and Type B TDA was used in the backfill. In a large steel soil box, a 1.07 m thick compacted soil layer was first built at the bottom. The concrete retaining wall 2.36 m in width, 2.69 m in length, and 2.21 m in height which had been constructed on site, was then placed on the top of the bottom soil layer. Type B TDA was compacted at the back of the retaining wall for 1.45 m thickness, and a 0.61 m thick soil layer was built on the top of the TDA layer. At the far end of the backfill, styrofoam blocks and bentonite bags were installed between the backfill and the soil box to minimize the rebounding forces exerted to the backfill. Input excitations used in the test include white noise, sine sweep, and earthquake

strong motions: Northridge, Kocaeli, and Takatori earthquakes. The shake table test started with a white noise excitation, followed by four events of sine sweep excitations and fourteen earthquake strong motions. The white noise excitation having a 3% root mean square amplitude lasted for 5 min. In the sine sweep excitations, excitation frequencies changed from 1 to 20 Hz and then from 20 to 1 Hz with two different amplitudes of 0.05 g and 0.075 g at the maximum. Three earthquake strong motions were applied with four different intensities changing from 25% to 100% by a 25% increment as the intensity was measured by the maximum acceleration. The last two excitations were 150% and 200% intensity Northridge earthquakes. The test results were then compared with previously available field test results from 2009 where retaining wall of same dimension was backfilled with conventional soil. The results showed that, the retaining wall with TDA backfill displaced more although less dynamic pressure was exerted on the wall by the TDA layer, the cumulative residual deformation showed that the TDA backfill experienced significantly larger residual shear deformation than the conventional soil backfill, indicating different failure planes developed in the backfill and the topsoil layer experienced larger lateral displacements and generated greater dynamic pressure on the wall. Considering the benefit of using TDA, the topsoil layer shall be strengthened with additional reinforcement such as geogrid to reduce movement.

In 2012 Xiao et al., carried out research on seismic responses of geo-synthetically reinforced walls with TDA and granular backfills. The MSE walls were constructed and tested on a shake table, which is housed in the structural laboratory in the Lyles College of Engineering at Fresno State. The table replicates ground motions that may be observed in actual earthquakes. The dimensions of the shaking table are 2.44 × 2.13 m (8 × 7 ft),

and the load capacity is 177.9 KN. The table is driven in one dimension by a 100 gallons-per-minute pump and an actuator that provides a 245 KN hydraulic fluid driving force through a 25.4 cm displacement stroke. The wall was 1.60 m tall, 1.68 m wide, and the horizontal depth (in the shaking direction) was 1.50 m. Two backfill materials were used. One was TDA that was manufactured by West Coast Rubber Recycling with the nominal size of 15.2 cm. The TDA had exposed steel beltings. The other was a poorly graded sand with no clay. It is observed that TDA is not compactable, compaction forces only temporarily compress the TDA, which rebounds after the compression force is removed. Therefore, the TDA was dumped into the box using a crane and leveled using shovels, then two people simply step evenly on the TDA. For sand backfill, a 15-kg hand hammer with a long handle and 30 × 30 cm steel base is used to compact the pre-moistened sand. To simulate the surcharge on the MSE wall, a concrete slab of 15 cm in thickness is anchored on top of the backfill, providing a uniform pressure of 3.38 KN/m^2. The potentiometers were fixed on an inertial frame outside of the shake table, and an inelastic wire connects to each potentiometer and to the geogrid of each layer. The potentiometers were spring loaded, but the spring force is significantly smaller than the seismic force, therefore, the spring stiffness did not affect the responses of the walls. The vertical deformation of the MSE wall during the shaking was measured using LVDT transducers that are anchored on the shake table above the concrete slab. Lateral displacements of the wall face, vertical settlement of the MSE wall surface, accelerations of the four layers within the MSE wall, and dynamic vertical stresses of the four layers within the MSE wall were analysed. Under the same seismic condition and the same wall configurations, the reinforced TDA wall behaves better than the conventional MSE wall. The advantages of

TDA backfill over sand includes less lateral displacement, less vertical settlement, less acceleration, apparent acceleration attenuation toward the top of the wall, and less static and dynamic stresses in the TDA backfill.

Srestha and Ravichandran (2018) conducted a study using a cantilever gravity retaining wall with a design height of 6.5 m with horizontal backfill surfaces in the front and back. Two backfill cases were considered here, one being traditional granular backfill and other being TDA backfill. The objective of the geotechnical design was to determine the appropriate lengths of toe and heel of the footing for the given material and loading conditions. Although the size of the tire aggregate ranges between 12 and 305 mm, only the size between 50 and 150 mm was considered suitable for use as a retaining wall backfill in this study to maintain the uniformity in backfill without additional effort. The mean values of the unit weight, friction angle and cohesion were taken to be 6.3 KN/m^3, 23° and 6.8 KN/m^2 respectively. The values of these properties are well within the range suitable for a material to be used as a retaining wall backfill. The in-situ soil was assumed to be a fine-grained soil with a unit weight of 18.07 KN/m^3, a friction angle of 28°, and a cohesion of 20 KN/m^2. The conventional granular backfill material was assumed to have a unit weight of 18.85 KN/m^3, a cohesion of zero, and a friction angle of 34°. The geotechnical design of the retaining wall for static loading condition was performed following the Allowable Stress Design procedure. The Coulomb earth pressure theory was used to compute the active and passive earth pressures acting on the wall. Several trial designs were conducted until the computed factors of safety against the key failure modes such as overturning, sliding, and bearing were satisfactory. The final static design that meets the design requirements consisted of the toe and heel lengths of 0.93 and

1.73 m, respectively, for the granular soil backfill and 1.53 and 0.91 m, respectively, for the tire aggregate backfill. The corresponding factors of safety against overturning, sliding, and bearing were 2.32, 2.15 and 3.12, respectively, for the granular soil backfill and 2.03, 2.86 and 5.71, respectively, for the tire aggregate backfill. The static analyses of retaining wall backfilled with in- situ soil and TDA were then studied using an advanced finite element program called PLAXIS. Based on the conventional geotechnical design, it is observed that the retaining wall with tire aggregate backfill is economical than conventional granular backfill in both static and dynamic conditions. Tire aggregate backfill provides a significant reduction in the volume of concrete required for constructing the retaining wall, volume of excavation and volume of backfill materials. From the computer simulations with only horizontal ground motion, it is observed that the tire aggregate induced lower shear force and bending moment for the entire length of the stem compared to the granular soil backfill. The results of the design and computer simulations justify that the tire aggregate can be a cost-effective alternative for conventional granular soil backfill. However, the shear force induced along the footing by granular soil backfill is lower compared to that induced by tire aggregate backfill. Further, the bending moment produced due to tire aggregate is higher along the toe and lower along the heel side of the footing compared to that produced by the granular soil.

In 2018, Djadouni et al., presented a study to compare the energy consumption, greenhouse gas emissions, and environmental damages for two methods of constructing retaining structures, one with backfilling retaining wall using sand and other method involving a retaining wall backfilled with shredded tires. The design of the two retaining walls of height 11 feet was taken from a study by Cecich et al. (1996). Considering the

extraction and production of the construction materials used, loading, transport and installation, the cumulative energy demand (CED) is determined for each construction method. The global warming potential (GWP), acidification potential (AP), Human Health Criteria Air-mobile, aquatic eutrophication potential, ozone depletion potential, and smog potential have been considered in addition to the CED. From the results obtained, they concluded that when RW is backfilled with shredded tires it requires 25 m^3 of concrete and 1.01 T of reinforcing steel. Furthermore, the retaining structure with shredded tires required approximately 189 m^3 of scrap tires to be shredded, transported, and installed. All this was proven to consume considerably less energy than the traditional solution, which involved the production, transportation, and installation of 30.75 m^3 of concrete, approximately 2.92 T of reinforcing steel, and 303 m^3 of sand. In this process, concrete, reinforcing steel, and sand transport contributed considerably to the higher CED of the traditional method. It was found that CED while using tire chips was 1.63 times lower than conventional backfill approach. Similarly, the results for GWP, AP, Human Health Criteria Air-mobile, aquatic eutrophication potential, ozone depletion potential, and smog potential were found to be lower for retaining wall backfilled with tire shreds. Thus, the use of shredded tires as retaining wall backfill leads to lower environmental impacts in terms of acidification, eutrophication, ozone depletion, photochemical smog, and human health particulates, compared to the traditional solution. The benefits of the shredded tires solution in comparison with the traditional solution can be mainly ascribed to the reduced demand for concrete and reinforcing steel by saving 18.69% of concrete and 65.47% of reinforcement steel, which causes considerably lower CED, CO2, and other polluting emissions.

2.6 Summary

To summarize, the literature review has explored the design and analysis of retaining wall, the potential of Tire Derived Aggregate (TDA) as a sustainable backfill material in retaining wall construction, and the application of Finite Element Analysis (FEA) in retaining wall design. The key findings from this chapter suggest that, retaining walls are critical structures that require careful design and analysis as it is subjected to a wide range of factors including soil properties, loading conditions, drainage and environmental considerations to ensure optimal performance, stability and safety.

Furthermore, the review has highlighted the potential benefits of using sustainable materials like Tire Derived Aggregate (TDA) in retaining wall construction, which can help reduce environmental impacts and promote more sustainable geotechnical engineering practices. In addition to that, the benefit of Finite Element Analysis (FEA) in simulating retaining wall behavior and design is also covered in this chapter.

CHAPTER 3 DEVELOPMENT OF TWO-DIMENSIONAL FINITE ELEMENT MODEL FOR RETAINING WALL BACKFILLED WITH TIRE DERIVED AGGREGATES

3.1 Introduction

Retaining walls are critical structures in geotechnical engineering. They are critical components of infrastructure projects, serving as barriers that prevent soil erosion, stabilize slopes, and support vertical or near-vertical grade changes. Thus, the selection of appropriate backfill materials for retaining walls is crucial to ensure structural integrity, long-term stability, and efficient performance of the wall. Traditional backfill materials, such as natural sands, have been widely used in construction projects. However, the ever-increasing need for sustainable practices and the desire to minimize environmental impact has led to a growing interest in exploring alternative materials for construction applications (Kumar and Parihar, 2023).

This study aims to investigate the performance of a retaining wall backfilled with Tire Derived Aggregate (TDA), a sustainable alternative to traditional backfill materials. By re-using scrap tires, this study aims to address two significant challenges simultaneously, the reduction of waste generated by tires as they reach the end of their useful life and the sustainability of construction practices. By evaluating these backfill material's geotechnical properties and performance, this study seeks to provide valuable insights into their behaviour and assess their potential as viable alternatives to conventional backfill materials.

While there is an environmental advantage to using recycled tires as TDA, a primary factor in selecting the material for use in civil engineering projects is the low unit weight of the aggregate. Often, during construction, poor-quality soils are encountered and can sustain only moderate loads before failure. By substituting TDA as backfill, the overburden stress is reduced. Additionally, TDA has a much lower active earth pressure coefficient, which can significantly reduce the design requirements for retaining walls. Since the TDA is essentially buried in the ground during construction, there is always a concern about groundwater contamination (Amirkhanian and Skelton, 2021).

When TDA is used as a fill for retaining wall, roadway, embankment, and railroad construction, TDA is placed above the water table, but there are only some instances where the TDA will be placed below the water table. For both above and below water table applications, the preponderance of evidence shows that TDA will not cause primary drinking water standards to be exceeded for metals. Moreover, TDA is unlikely to increase levels of metals with primary drinking water standards above naturally occurring background levels. Based on several experimental studies conducted TDA used as fill in above groundwater table applications would be expected to have negligible human health-based effects on drinking water quality or aquatic toxicity effects on freshwater species (Humphrey and Swett, 2006).

For the design of TDA fills and backfills, conventional procedures for soil have been adopted to provide designers with a simple, convenient method, which includes the Mohr–Coulomb failure criterion. Past projects demonstrated that such methods could be successfully used in TDA backfill construction precisely, under static loadings (Ahn and Cheng, 2014).

This study aims to investigate the performance of retaining wall backfilled with TDA. A comprehensive Finite Element Analysis is conducted to model the TDA backfilled retaining wall to predict the earth pressure on the wall. The validity of the finite element model is demonstrated through a case study, where the predicted results are compared to actual field test measurements, ensuring the reliability and accuracy of the analysis.

3.2 Case Study

Hemanata Hazarika in 2005, carried out a series of field test experiment in Japan to investigate the effect of using a tire-chip cushion as a compressible inclusion between a rigid non-yielding retaining wall and backfill. This field test results are used here for validation by developing a replica of the model in PLAXIS 2D software. The retaining wall is modeled during backfilling, using the methodology given in the following sections. This analysis was used to determine the performance of the model and to check the validity and accuracy of the proposed model. To examine the effect of Tire Derived Aggregate (TDA) on retaining wall, the analysis is carried out under two different conditions. Two models of retaining wall are investigated here, where one is backfilled using Soma No. 6 sand, whereas the other wall is backfilled by placing a cushion of tire-chips of 30cm thickness between the retaining wall and Soma No. 6 backfill sand. In both the cases, the retaining wall installed was of 1.5m height. Additionally, a surcharge of 8.3KN/m^2 was then applied to the sand from above in both the cases for a length of 1.4m on both sides of the wall and the earth pressure on the wall was measured by installing earth pressure cells of diameter 10cm which were placed at 30cm intervals along the

height of the wall. Figure 3.1 and 3.2 shows the overview of experimental setup in both the case 1 and case 2.

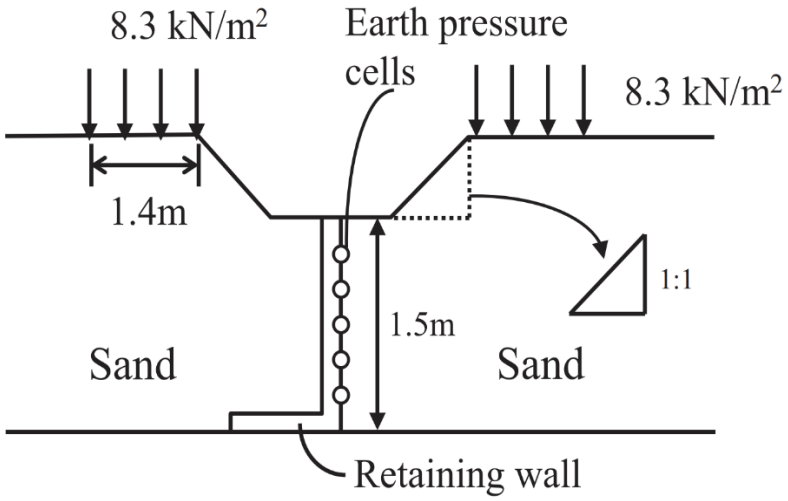

Fig 3.1 Experimental setup of retaining wall backfilled with sand (Hazarika et al., 2005)

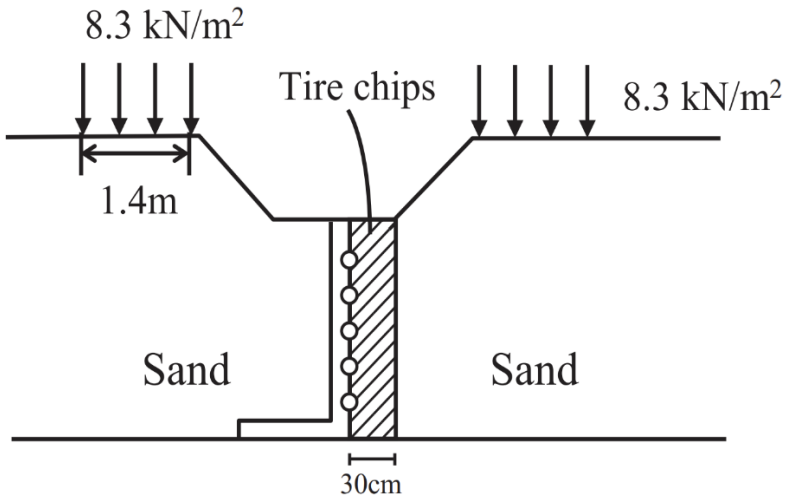

Fig 3.2 Experimental setup of retaining wall backfilled with tire chips and sand (Hazarika et al., 2005)

3.3 Finite Element Model (FEM) Development

PLAXIS 2D is the finite element analysis software used here which is specifically designed for geotechnical engineering applications.

3.3.1 Material Properties

- **Concrete**

The concrete of the retaining wall was designed as Linear Elastic Model to simulate the behavior of concrete, which is assumed to be a linear elastic material, as it simplifies the analysis, allowing efficient and accurate results. Linear elastic models are suitable for serviceability limit states, where the structure is expected to behave elastically under normal loads. Additionally, linear elastic models are useful for initial design and feasibility studies, which in turn provides a quick estimate of the structure's behavior. Moreover, material properties of concrete such as young's modulus and Poisson's ratio are well defined and readily available, making linear elastic model more convenient.

In the context of PLAXIS 2D materials model manual (2021), Material models are generally expressed as a relationship between infinitesimal increments of effective stress (effective stress rates) and infinitesimal increments of strain (strain rates). This relationship may be expressed in the form as:

$$\sigma' = M\,\mathcal{E}$$

Where, σ′ is the effective stress rate, Ɛ is the strain rate and M is a material stiffness matrix.

Linear elastic model is the simplest material model in PLAXIS and is based on Hooke's law for isotropic linear elastic behaviour. Hooke's law can be given by the following equation:

$$\begin{vmatrix} \sigma' \\ \sigma' \\ \sigma' \\ \sigma' \\ \sigma' \\ \sigma' \end{vmatrix} = \frac{E'}{(1-2\nu')(1+\nu')} \begin{vmatrix} 1-\nu' & \nu' & \nu' & 0 & 0 & 0 \\ \nu' & 1-\nu' & \nu' & 0 & 0 & 0 \\ \nu' & \nu' & 1-\nu' & 0 & 0 & 0 \\ 0 & 0 & 0 & \frac{1}{2}-\nu' & 0 & 0 \\ 0 & 0 & 0 & 0 & \frac{1}{2}-\nu' & 0 \\ 0 & 0 & 0 & 0 & 0 & \frac{1}{2}-\nu' \end{vmatrix} \begin{vmatrix} \varepsilon_{xx} \\ \varepsilon_{yy} \\ \varepsilon_{zz} \\ \gamma_{xy} \\ \gamma_{yz} \\ \gamma_{zx} \end{vmatrix}$$

Two parameters are used in this model, the effective Young's modulus, E', and the effective Poisson's ratio, ν'. According to Hooke's Law, the relationship between Young's modulus E and other stiffness moduli, such as the shear modulus G, the bulk modulus K, and the oedometer modulus E_{oed}, is given by:

$$G = \frac{E}{2(1+\nu)}$$

$$K = \frac{E}{3(1-2\nu)}$$

$$E_{oed} = \frac{(1-\nu)E}{(1-2\nu)(1+\nu)}$$

During the input of material parameters for the Linear Elastic model for concrete the values of G and E_{oed} are presented as auxiliary parameters (alternatives), calculated from the above equations. But the alternatives are influenced by the input values of E and ν.

Entering a particular value for one of the alternatives G or E_{oed} results in a change of the E modulus. The Linear Elastic model is usually inappropriate to model the highly non-linear behaviour of soil, but it is of interest to simulate structural behaviour, such as thick concrete walls or plates, for which strength properties are usually very high compared with those of soil (PLAXIS 2D materials model manual, 2021). The following table 3.1 shows the input parameters adopted for the concrete material in this study.

Table 3.1 Input parameters of concrete material

Material	Concrete
Material Model	Linear Elastic
Unsaturated unit weight (γ_{unsat})	24 KN/m^3
Saturated unit weight (γ_{sat})	24 KN/m^3
Elastic Modulus (E)	50000 KN/m^2
Poisson's ratio (v')	0.3
R_{inter}	0.3

- **Backfill Sand**

The backfill sand of retaining wall was designed as a Mohr-Colomb model because sand exhibits frictional and cohesive behavior which can be accurately captured by this model. Although sand has low cohesion, this Mohr-Colomb model considers it, ensuring a more accurate representation of sand behavior. Moreover, angle of friction (ϕ) of sand is a critical parameter in retaining wall design, which is precisely accounted in Mohr-Colomb model. Furthermore, this model accounts for non-linear behavior, which is essential for sand under various stress conditions.

In the context of PLAXIS 2D materials model manual (2021), the Mohr-Coulomb yield condition is an extension of Coulomb's friction law to general states of stress. In fact, this condition ensures that Coulomb's friction law is obeyed in any plane within a material element. Figure 3.3 presents Mohr-Coulomb yield surface in principle stress space. The full Mohr-Coulomb yield condition consists of six yield functions (f) when formulated in terms of principal stresses as follows:

$$f_{1a} = \frac{1}{2}(\sigma'_2 - \sigma'_3) + \frac{1}{2}(\sigma'_2 + \sigma'_3)\sin\emptyset - c\cos\emptyset \leq 0$$

$$f_{1b} = \frac{1}{2}(\sigma'_3 - \sigma'_2) + \frac{1}{2}(\sigma'_3 + \sigma'_2)\sin\emptyset - c\cos\emptyset \leq 0$$

$$f_{2a} = \frac{1}{2}(\sigma'_3 - \sigma'_1) + \frac{1}{2}(\sigma'_3 + \sigma'_1)\sin\emptyset - c\cos\emptyset \leq 0$$

$$f_{2b} = \frac{1}{2}(\sigma'_1 - \sigma'_3) + \frac{1}{2}(\sigma'_1 + \sigma'_3)\sin\emptyset - c\cos\emptyset \leq 0$$

$$f_{3a} = \frac{1}{2}(\sigma'_1 - \sigma'_2) + \frac{1}{2}(\sigma'_1 + \sigma'_2)\sin\emptyset - c\cos\emptyset \leq 0$$

$$f_{3b} = \frac{1}{2}(\sigma'_2 - \sigma'_1) + \frac{1}{2}(\sigma'_2 + \sigma'_1)\sin\emptyset - c\cos\emptyset \leq 0$$

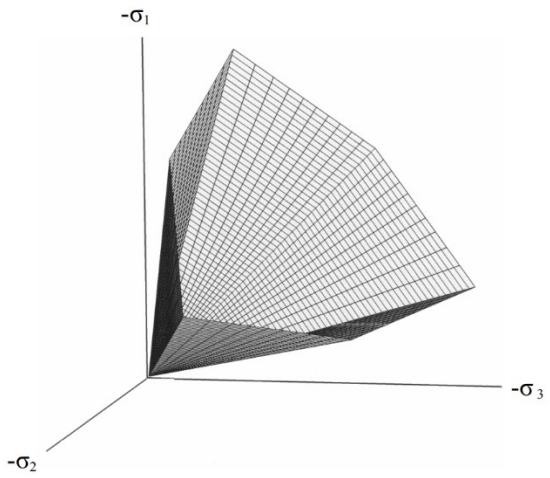

Fig 3.3 The Mohr-Coulomb yield surface in principal stress space for no cohesion (PLAXIS 2D materials model manual, 2021)

In addition to the yield functions, the six plastic potential functions (g) are defined for the Mohr-Coulomb model are as follows:

$$g_{1a} = \frac{1}{2}(\sigma'_2 - \sigma'_3) + \frac{1}{2}(\sigma'_2 + \sigma'_3)\sin\psi$$

$$g_{1b} = \frac{1}{2}(\sigma'_3 - \sigma'_2) + \frac{1}{2}(\sigma'_3 + \sigma'_2)\sin\psi$$

$$g_{2a} = \frac{1}{2}(\sigma'_3 - \sigma'_1) + \frac{1}{2}(\sigma'_3 + \sigma'_1)\sin\psi$$

$$g_{2b} = \frac{1}{2}(\sigma'_1 - \sigma'_3) + \frac{1}{2}(\sigma'_1 + \sigma'_3)\sin\psi$$

$$g_{3a} = \frac{1}{2}(\sigma'_1 - \sigma'_2) + \frac{1}{2}(\sigma'_1 + \sigma'_2)\sin\psi$$

$$g_{3b} = \frac{1}{2}(\sigma'_2 - \sigma'_1) + \frac{1}{2}(\sigma'_2 + \sigma'_1)\sin\psi$$

The plastic potential functions contain a third plasticity parameter, the dilatancy angle ψ. This parameter is required to model positive plastic volumetric strain increments (dilatancy) as actually observed for dense soils.

For $c > 0$, the standard Mohr-Coulomb criterion allows for tension. In fact, allowable tensile stresses increase with cohesion. Soil can sustain none or only very small tensile stresses. This behaviour can be included in a PLAXIS analysis by specifying a tension cut-off. In this case, Mohr circles with positive principal stresses are not allowed. The tension cut-off introduces three additional yield functions (f), defined as:

$$f_4 = \sigma'_1 - \sigma_t \leq 0$$

$$f_5 = \sigma'_2 - \sigma_t \leq 0$$

$$f_6 = \sigma'_3 - \sigma_t \leq 0$$

When this tension cut-off procedure is used, the allowable tensile stress (σ_t) is, by default, taken equal to zero. For these three yield functions, an associated flow rule is adopted. For stress states within the yield surface, the behaviour is elastic and obeys Hooke's law for isotropic linear elasticity. Hence, besides the plasticity parameters c, ϕ, and ψ, input is required on the elastic Young's modulus (E) and Poisson's ratio (ν) for modeling sand as Mohr-Colomb model (PLAXIS 2D materials model manual, 2021).The following table

3.2 shows the input parameters adopted for the sand material in this study and these parameters were taken from Hazarika's (2005) study.

Table 3.2 Input parameters of sand model

Material	Sand
Material Model	Mohr-Colomb
Unsaturated unit weight (γ_{unsat})	16.6 KN/m^3
Saturated unit weight (γ_{sat})	16.6 KN/m^3
Elastic Modulus (E)	56000 KN/m^2
Poisson's ratio (v')	0.3
Cohesion (c')	2 KN/m^2
Angle of friction (ϕ)	40^0
Dilatancy angle (ψ)	10^0
R_{inter}	0.3

- **Tire Derived Aggregate (TDA) Model**

The Tire derived aggregate (TDA) as retaining wall backfill was modeled as Hardening soil model in PLAXIS 2D. TDA exhibits soil like behavior under various stress conditions and undergoes compression and settlement due to applied loads, all which can be

accurately captured by hardening soil model. The Hardening Soil model is an advanced model for simulating the behaviour of different types of soil, both soft soils and stiff soils, Schanz (1998). The Hardening-Soil model uses the theory of plasticity rather than the theory of elasticity. Some basic characteristics of this model are stress dependent stiffness (m), reference stiffness modulus (E_{50}^{ref}), oedometer stiffness modulus (E_{oed}^{ref}), unloading-reloading modulus (E_{ur}^{ref}), cohesion (c), angle of friction (ϕ) and dilatancy angle (ψ).

In the context of PLAXIS 2D materials model manual (2021), a basic idea for the formulation of hardening soil model is the hyperbolic relationship between the vertical strain (ε_1), and the deviatoric stress (q) in primary triaxial loading. Here standard drained triaxial tests tend to yield curves that can be described as:

$$-\varepsilon_1 = \frac{1}{E_i} - \frac{q}{1 - q/q_a} \quad \text{, for } q < q_f$$

Where qa is the asymptotic value of the shear strength and E_i the initial stiffness, which is equal to,

$$E_i = \frac{2\,E_{50}}{2 - R_f}$$

The parameter E_{50} is the confining stress dependent stiffness modulus for primary loading and is given by the equation:

$$E_{50} = E_{50}^{ref}\left(\frac{c\,\cos\varphi - \sigma_3'\sin\varphi}{c\,\cos\varphi + p^{ref}\sin\varphi}\right)^m$$

Where $'E_{50}^{ref}{}'$ is the reference stiffness modulus, 'm' is the power and 'p^{ref}' is the reference confining pressure. In PLAXIS, a default setting p^{ref} is set at 100 KN/m^2. The amount of

stress dependency is given by the power m. In order to simulate a logarithmic compression behavior, the value of power (m) should be in the range of 0.5<m<1. The oedometer stiffness is defined as:

$$E_{oed} = E_{oed}^{ref}\left(\frac{c\ \cos\varphi - \sigma_1' \sin\varphi}{c\ \cos\varphi + p^{ref} \sin\varphi} \right)^m$$

Where 'E_{oed}^{ref}' is the oedometer stiffness modulus, 'm' is the power and 'p^{ref}' is the reference confining pressure. For, unloading and reloading stress path, another stress dependant stiffness modulus should be used:

$$E_{ur} = E_{ur}^{ref}\left(\frac{c\ \cos\varphi - \sigma_3' \sin\varphi}{c\ \cos\varphi + p^{ref} \sin\varphi} \right)^m$$

Where 'E_{ur}^{ref}' is the unloading-reloading modulus, 'm' is the power and 'p^{ref}' is the reference confining pressure. As per the default settings used in PLAXIS, E_{ur}^{ref} is equal to 3 times of E_{50}^{ref}. The advantage of the Hardening Soil model over the Mohr-Coulomb model is, when using the Mohr-Coulomb model the user must select a fixed value of Young's modulus whereas for real soil this stiffness depends on stress levels. It is therefore necessary to estimate the stress levels within the soil and use these to obtain suitable values of stiffness. With the Hardening Soil model, however, this cumbersome selection of input parameters is not required. Instead, a stiffness modulus E_{50}^{ref} is defined uses p^{ref} as 100 stress units. The following table 3.3 shows the input parameters adopted for the TDA model in this study and these parameters were taken from the study done by Mahgoub and El Naggar (2019).

Table 3.3 Input parameters of TDA model

Material	Tire Derived Aggregate
Material Model	Hardening Soil Model
Unsaturated unit weight (γ_{unsat})	6.3 KN/m^3
Saturated unit weight (γ_{sat})	6.3 KN/m^3
Reference stiffness modulus (E_{50}^{ref})	2750 KN/m^2
Oedometer stiffness modulus (E_{oed}^{ref})	2200 KN/m^2
Unloading-reloading modulus (E_{ur}^{ref})	8250 KN/m^2
Power (m)	0.95
Cohesion (c')	24 KN/m^2
Angle of friction (ϕ)	26.50^0
R_{inter}	0.65

3.3.2 Modeling Interface Elements

While modeling retaining wall in PLAXIS 2D, it is important to note that retaining walls interact with surrounding soil, which affects their behavior. Interface elements are used to simulate this interaction by capturing the exchange of forces and displacements between the soil and the structure. Without an interface the structure and the soil are tied together with no relative displacement could be possible between structure and soil. By using an interface, node pairs are created at the interface of structure and soil. From a node pair, one node belongs to the structure and the other node belongs to the soil. The

interaction between these two nodes consists of two elastic-perfectly plastic springs. One elastic-perfectly plastic spring to model the gap displacement and one elastic-perfectly plastic spring to model slip displacement (PLAXIS 2D manual, 2012). In this study, interface elements were provided around the retaining wall to study the interaction between the wall and soil, also allowing the movement of the wall. The following figure 3.4 represents an example for connectivity plot of soil-structure connection with and without an interface.

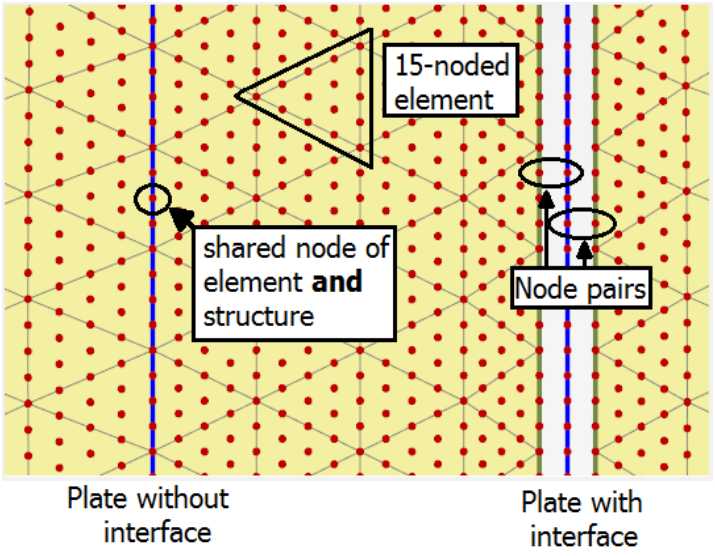

Fig 3.4 Connectivity plot of a soil-structure connection with and without interface (PLAXIS 2D manual, 2012)

3.3.3 Mesh

In PLAXIS 2D, while generating the mesh for the modeled structure, the geometry is divided into elements of the basic element type and compatible structural elements. The mesh generation takes full account of position of points and lines in the model, so that the

exact position of layers, loads and structures are accounted for the finite element mesh. This generation process is based on a robust triangulation principle that searches for optimized triangles (PLAXIS 2D manual, 2021).

The finite element model (FEM) for retaining wall in both cases, backfilled without and with Tire Derived Aggregate (TDA) was developed by setting the mesh coarseness to be very fine, because they provide accurate results as they can capture the behavior of soil and stress distribution better.

3.3.4 Boundary Conditions

The boundary conditions were set to be default in the study. In the model, the boundary condition was set to be 'normally fixed' in the horizontal direction (for X_{min} and X_{max}) and in the vertical direction the base was set to be 'fully fixed' (for Y_{min}) whereas the top was set to be 'free' (for Y_{max}).

3.3.5 Model geometry

The geometry of the retaining wall built in PLAXIS 2D, was same as that used by Hemantha Hazarika (2005) in his field experiment. Though a retaining wall with backfill on both sides equally up to the height of the wall is not a common setup practice, it was used in the experimental setup by Hazarika to create a symmetrical model. Figure 3.5 represents the geometry of the model of retaining wall for case 1 and case 2 of Hazarika's study.

- Case 1

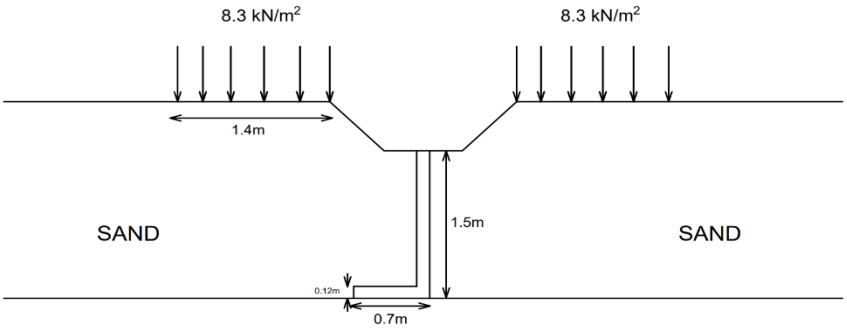

- Case 2

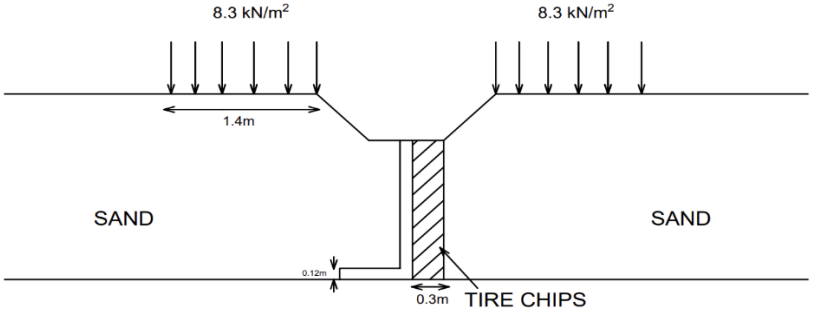

Fig 3.5 Geometry of the model for case 1 and case 2

3.3.6 Staged Construction

Staged construction is the approach used in PLAXIS 2D where structures are built in stages to accommodate complex construction sequences, soil structure interaction and settlement behavior.

Initial Phase: The initial phase was performed by gravity loading technique, which applies the weight of soil and structure as initial load and the initial state stress including the geostatic stress was established. The ground water table (GWT) was not considered in the study. The concrete retaining wall structure, interfaces along with backfill sand and tire derived aggregate was activated in this stage of analysis. The following figures 3.6 and 3.7 shows the initial phase stage in both the cases of study.

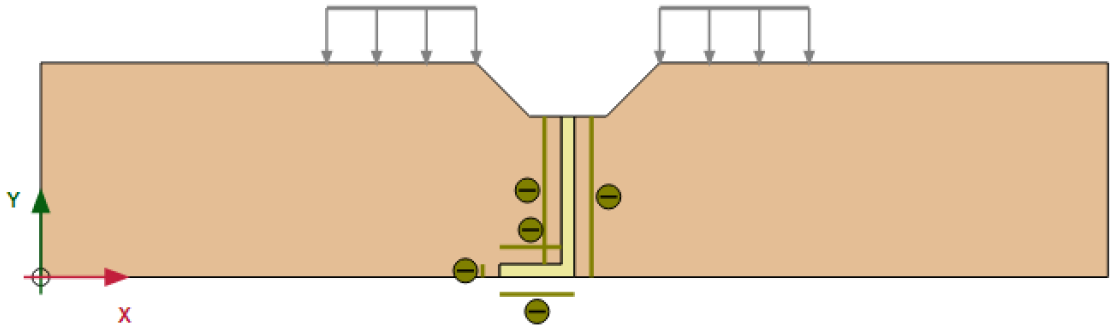

Fig 3.6 Case 1: Initial phase of retaining wall backfilled with sand only

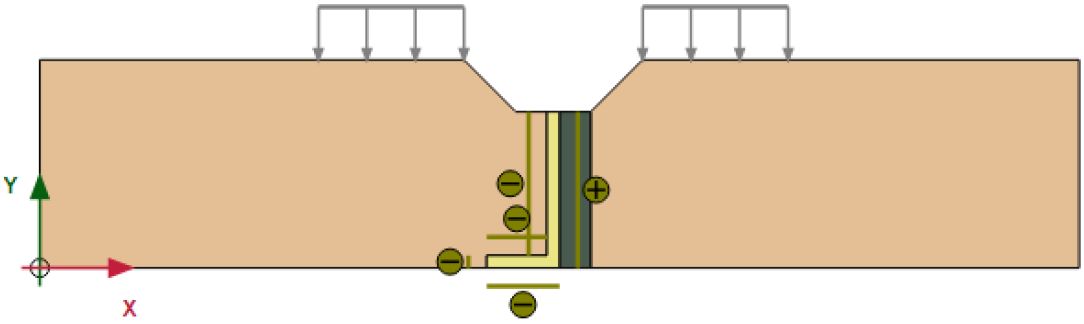

Fig 3.7 Case 2: Initial phase of retaining wall backfilled with sand and tire derived aggregates

Phase 1: The second stage stimulates the external surcharge of 8.3Kpa applied on both sides of the retaining wall above the sand for 1.4m. The surcharge on both sides of the wall was activated in this stage of construction. The following figures 3.8 and 3.9 shows the phase one stage in both the cases of study.

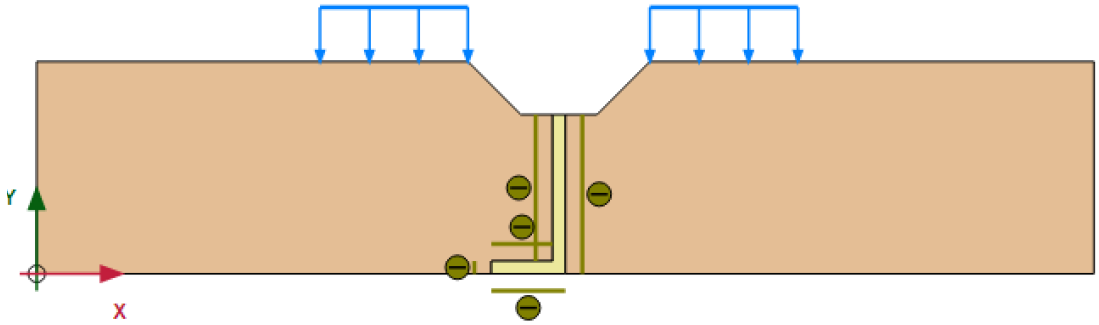

Fig 3.8 Case 1: Phase 1 of retaining wall backfilled with sand only

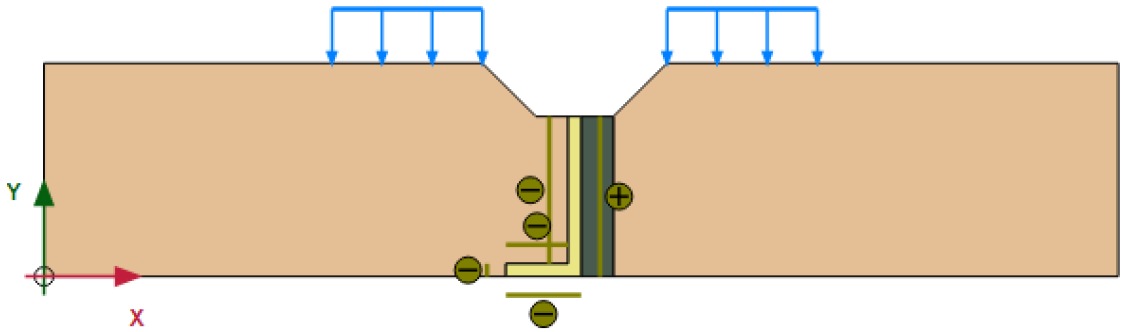

Fig 3.9 Case 2: Phase 1 of retaining wall backfilled with sand and tire derived aggregates

3.4 Results

This section presents the results and discussion of the finite element model analysis conducted in PLAXIS 2D to investigate the earth pressure of retaining wall backfilled with tire derived aggregate (TDA). The concurrence between the obtained results with the field test results proves the validity of the model.

The following figures 3.10 and 3.11 presents the comparison of earth pressure results obtained from PLAXIS 2D analysis and Hazarika et al., (2005) field study results:

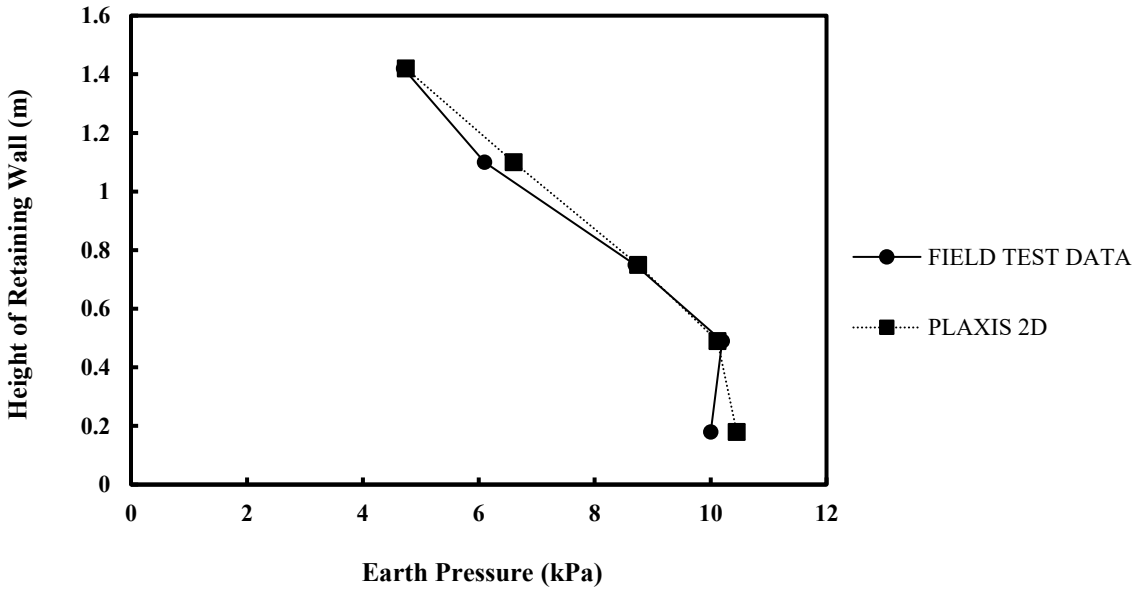

Fig 3.10 Earth pressure at retaining wall of Hazarika et al., (2005) field test result and PLAXIS 2D results of Case 1 backfilled with sand only

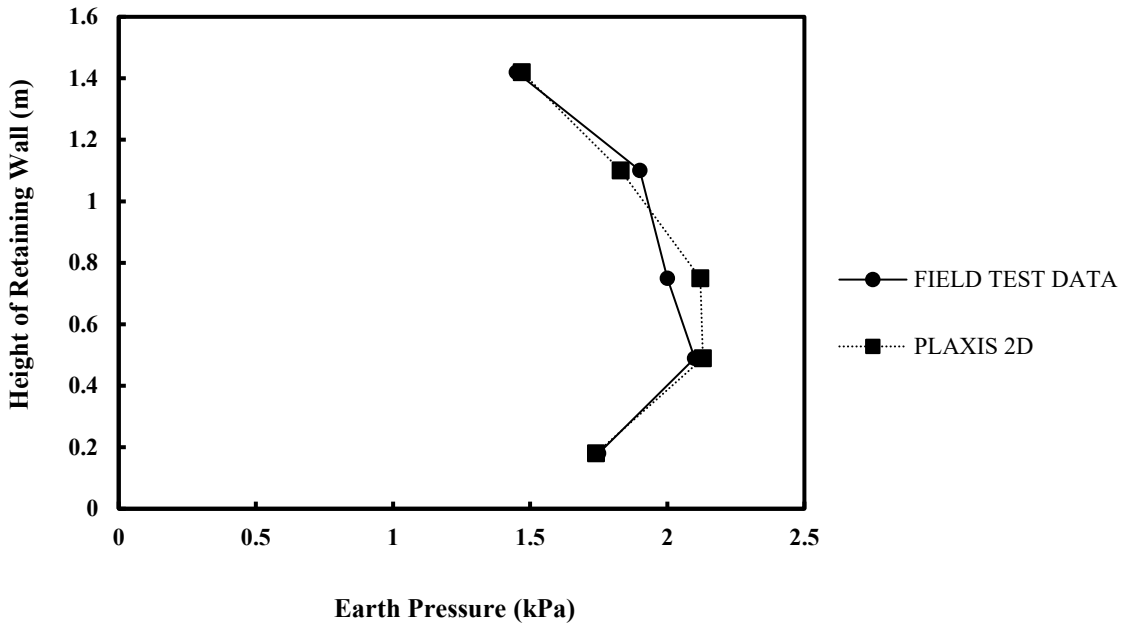

Fig 3.11 Earth pressure at retaining wall of Hazarika et al., (2005) field test result and PLAXIS 2D results of Case 2 backfilled with sand and tire derived aggregates

The comparison between the field test results and the PLAXIS 2D simulation results, as shown in the above graphs, demonstrates a remarkable concurrency. In Case 1 where retaining wall was backfilled with sand only, field test results showed an earth pressure of 10kPa at height 0.18m of the wall, at the same time PLAXIS 2D gave an earth pressure of 10.45kPa at the same height. Whereas, at the top of the wall in this case, at a height of 1.42m, earth pressure is found to lower and field test data gave 4.7kPa and PLAXIS 2D analysis showed 4.74kPa at the same height of the wall.

However, in Case 2 where retaining wall was backfilled with sand with inclusion of a 0.3m TDA layer, between the wall and sand, a significant reduction in earth pressure is

observed when compared to Case 1. In this case earth pressure of 1.75kPa was observed at the height of 0.18m of the wall for field test at the same time PLAXIS 2D results showed 1.74kPa. Whereas, at the top of the wall in this case, at a height of 1.42m, earth pressure is found to decrease and field test data gave 1.45kPa and PLAXIS 2D analysis showed 1.47kPa at the same height of the wall.

This concurrency validates the accuracy of the finite element model in capturing the reduction of earth pressure when tire derived aggregate is incorporated in the backfill of retaining wall. This concurrence also highlights the potential of using TDA as a backfill material.

From the study it is clear that the combination of sand and tire chips lowers the earth pressure than, when backfilled with conventional sand only. This reduction in earth pressure is achieved through a mechanism of simulating an intermediate active state. In the light of the results, it can be inferred that, when a buffer material with high compressibility like TDA is inserted between the wall and the backfill, a reduction in earth pressure of the retaining wall happens, as the soil in the vicinity of the wall enters an active or quasi-active state, in which it is deformed by the buffer, and when soil moves to the active state, the active earth pressure is reduced.

3.5 Conclusion

This chapter presented a study by comparing a retaining wall of height 1.5m backfilled with conventional sand only and with sand and tire derived aggregate (TDA). The earth pressure of the wall in both the cases was studied by a two-dimensional finite element analysis using the software PLAXIS 2D. The excellent agreement between the field test measurements and computational results confirms the accuracy and validity of the finite element model and the efficiency of TDA backfill. This study outlines the following conclusions:

- When tire derived aggregate is incorporated, a reduction in earth pressure is observed, as a result of the transitioning of backfill to active state. When three beneficial properties of TDA like, light unit weight, small stiffness and small Poisson's ratio are incorporated, the backfill soil easily approaches active state, and hence reduction in earth pressure against the wall can be observed.
- The successful validation of the 2D finite element model, as demonstrated by its accurate performance, provides a solid foundation for proceeding with a comprehensive parametric study in the subsequent chapters.

CHAPTER 4 PARAMETRIC STUDY OF RETAINING WALL BACKFILLED WITH TIRE DERIVED AGGREGATES

4.1 Introduction

This successful implementation of tire derived aggregate (TDA) as a backfill material in retaining wall, as demonstrated in the previous chapters, warrants further investigation to ensure its validity at larger scales. This chapter presents results from the parametric studies for retaining walls backfilled with tire derived aggregates (TDA). The parametric studies aim to verify the applicability of tire derived aggregate backfilled retaining wall design for larger infrastructure projects and to validate the numerical models and design assumptions used in the smaller scale studies discussed in the previous chapter.

Retaining walls are essential structures in geotechnical engineering, used to support soils or other materials and prevent erosion and landslides. The backfill material used in retaining walls plays a crucial role in their stability and performance. Traditional backfill materials, such as soil or aggregate can be heavy and may lead to high lateral earth pressures, which can compromise the structural integrity of the retaining wall. Whereas TDA is an essential substitute to conventional backfill materials because of its low unit weight and porous nature.

The parametric study was based on two-dimensional finite element analysis, which were carried out using the software PLAXIS 2D. It is a finite element software that simulates the behavior of geotechnical structures particularly for the analysis of soil-structure interaction problems like retaining walls. PLAXIS 2D can handle non-linear material

behavior, which is essential for modeling the stress-strain behavior of TDA which is a non-linear material. This software also has user friendly interface which makes it easier to define the problem, input data and input results. PLAXIS 2D provides a range of theoretical models to simulate material behavior including Mohr-Colomb, which is a classic model for soil failure, hardening soil model, which is an advanced model for soil hardening and softening, linear elastic model, which is a simplified model for soil deformation and stress analysis and many more. These theories enable the program to accommodate various soil types and behaviors, allowing for more accurate and comprehensive geotechnical analysis.

By scaling up the tire derived aggregate (TDA) backfilled retaining wall design, this chapter aims to bridge the gap between laboratory and field applications, by demonstrating the potential of TDA to be used in larger infrastructural projects.

4.2 Parametric study on scaled up model

Following the successful validation of tire derived aggregate (TDA) backfilled retaining wall model, this study takes a crucial step forward by investigating the behavior of a three-times scaled up model. This significant increase in scale allows for a more comprehensive understanding of the structural performance.

4.2.1 Model geometry

The following presents the geometry of the three – times scaled model of the retaining wall backfilled with tire derived aggregates (TDA). Along with the dimensions of the wall the surcharge applied on top of the sand was also multiplied to three times. Model was scaled up in order to identify the effect of TDA on retaining wall with larger heights. The following figure 4.1 represents the geometry of the scaled retaining wall.

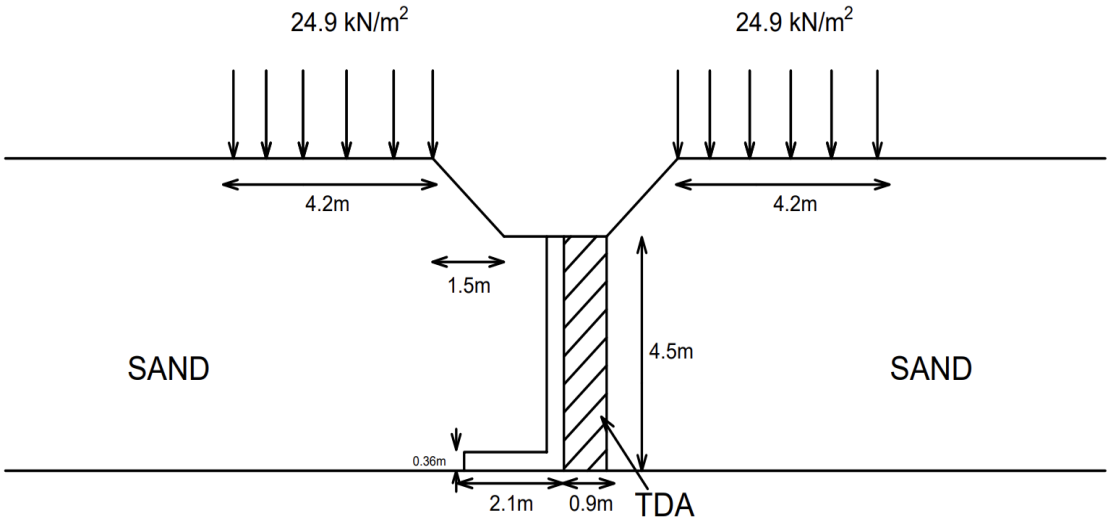

Fig 4.1 Geometry of the scaled model

4.2.2 Finite Element Model (FEM) Development

In this study, we utilized PLAXIS 2D, a specialized finite element analysis software tailored for geotechnical engineering applications. This section presents the material properties, mesh and boundary conditions used in this analysis.

- **Material Properties**

The following table presents the input properties of the materials used in this study, which are briefly described in the previous chapter.

Table 4.1 Input properties of the materials used

Material	Backfill sand	Tire Derived Aggregate (TDA)	Concrete
Material Model	Mohr-Colomb	Hardening Soil	Linear Elastic
Unsaturated unit weight (γ_{unsat})	16.6 KN/m^3	6.3 KN/m^3	24 KN/m^3
Saturated unit weight (γ_{sat})	16.6 KN/m^3	6.3 KN/m^3	24 KN/m^3
Elastic Modulus (E)	56000 KN/m^2	-	50000 KN/m^2
Reference stiffness modulus (E_{50}^{ref})	-	2750 KN/m^2	-
Oedometer stiffness modulus (E_{oed}^{ref})	-	2200 KN/m^2	-
Unloading-reloading modulus (E_{ur}^{ref})	-	8250 KN/m^2	-

Material	Backfill sand	Tire Derived Aggregate (TDA)	Concrete
Poisson's ratio (v')	0.3	-	0.3
Power (m)	-	0.95	-
Cohesion (c')	2 KN/m^2	24 KN/m^2	-
Angle of friction (ϕ)	40^0	26.5^0	-
Dilatancy angle (ψ)	10^0	-	-
R_{inter}	0.3	0.65	0.3

- **Interface Elements**

Interface elements are provided to simulate the soil-structure interaction by capturing the exchange of forces and displacements between the soil and the structure. Interface elements were provided around the retaining wall, which allowed the movement of wall and also captured the interaction between wall and surrounding soil.

- **Mesh and Boundary Conditions**

In this study, while generating the mesh for the modeled structure, the geometry is divided into elements of the basic element type and compatible structural elements. The finite element model (FEM) for retaining wall was developed by setting the mesh coarseness to be very fine.

Boundary conditions ensure accurate and reliable analysis results. They help define the extent of problem and what is being analysed. Incorrect or incomplete boundary conditions always leads to inaccurate analysis results. The boundary conditions were set to be by default in this study. In the model, the boundary condition was set to be 'normally fixed' in the horizontal direction (for X_{min} and X_{max}) and in the vertical direction the base was set to be 'fully fixed' (for Y_{min}) whereas the top was set to be 'free' (for Y_{max}).

- **Staged Construction**

The construction stages for the finite element model were simulated in PLAXIS 2D modeling. The initial stage was performed by gravity loading technique, where initial geo-static stresses were established. This technique applies the weight of soil and structure as initial load and hence calculates the initial state stress including the geostatic stress. The ground water table was not considered in the study. In this phase, the retaining wall, backfill sand, backfill TDA and interfaces were activated. In the next phase called as Phase 1, the external surcharge loads on both sides of the retaining wall above the sand were activated, and the boundary conditions remains the same in both the construction stages. After establishing the phases of construction, the calculation was done. The following figures 4.2 and 4.3 represents the different phases of this analysis.

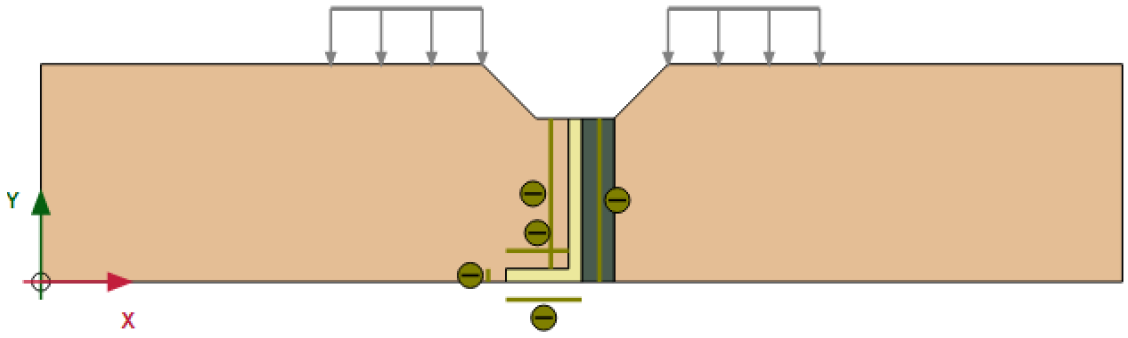

Fig 4.2 Initial phase of retaining wall backfilled with sand and tire derived aggregates

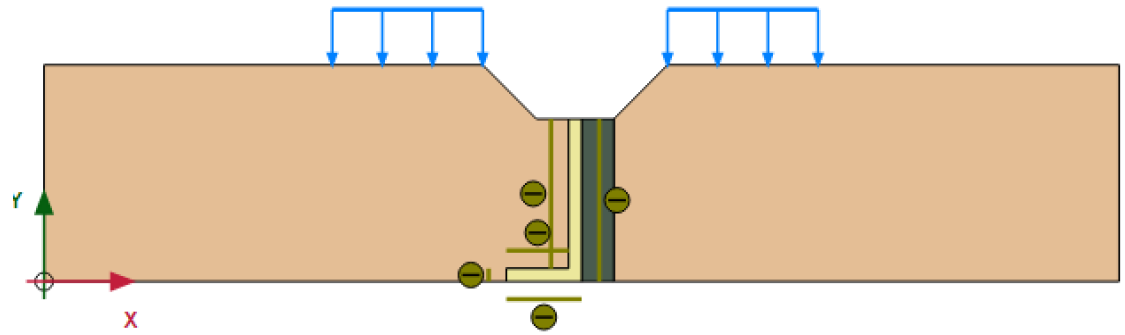

Fig 4.3 Phase 1 of retaining wall backfilled with sand and tire derived aggregates

4.2.3 Earth pressure analysis

The following figure 4.4 shows a graph plotted for the earth pressure results obtained from PLAXIS 2D analysis of the retaining wall of height 4.5m, thickness 0.36m with a surcharge load of 24.9kPa on both sides of the wall for a distance of 4.2m. An earth

pressure of 4.65kPa is observed at the bottom of the wall at a height of 0.56m and at the top of the wall earth pressure was measured to be 4.26kPa at a height of 4.28m.

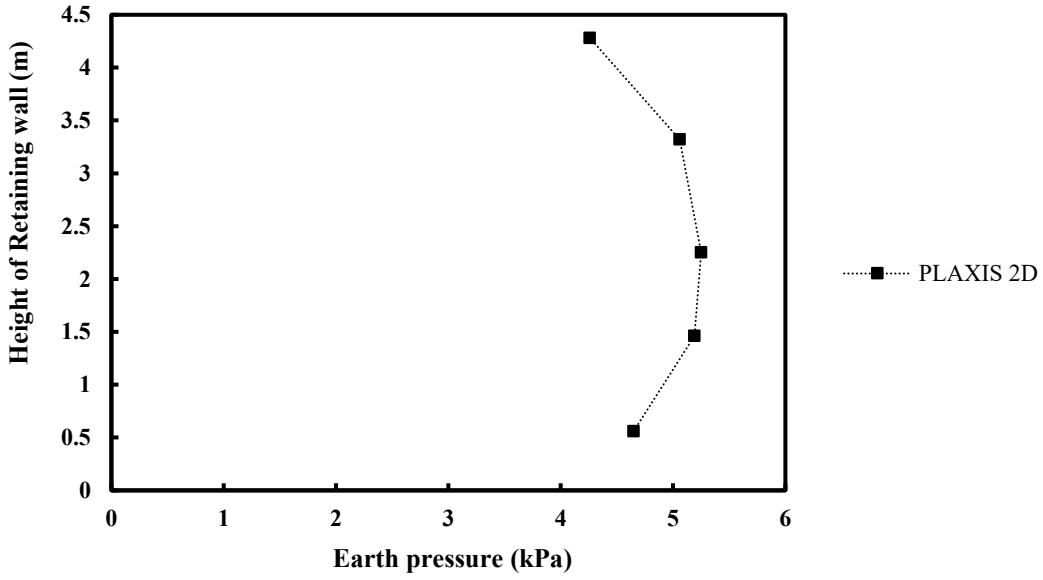

Fig 4.4 Earth pressure at scaled retaining wall backfilled with sand and tire derived aggregates

4.2.4 Comparison between the actual model and the scaled – up model

The actual model of the study was from Hazarika et., (2005) where retaining wall was of height 1.5m, thickness of the wall was 0.12m. In this study, three times scaled – up was used for the analysis with a height of 4.5m and wall thickness of 0.36m. To check the validity of the scaled model, normalised stress was calculated for the actual model of retaining wall and for the scaled model and compared. Normalised stress was calculated as the ratio of earth pressure on the retaining wall at a specific height to the corresponding

height of the wall at that point. Comparing the normalized stress between the actual model and the scaled model, the following graph was plotted. At the bottom of the wall, for the actual model of retaining wall, normalised stress was found to be 9.33kPa at a height of 0.19m, whereas for the scaled model it was found to be 8.27kPa at a height of 0.56m. However, at the top of the wall, normalised stress was found to be 1.03kPa at the height 1.43m for the actual model and 1kPa at the height of 4.28m for the scaled model.

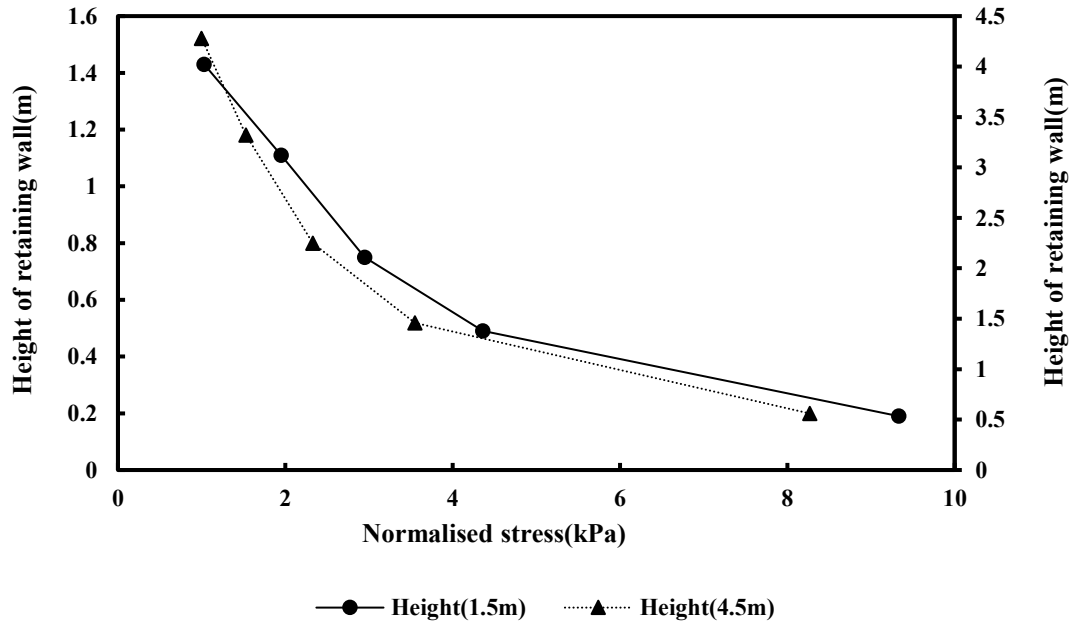

Fig 4.5 Normalized earth pressure in retaining wall backfilled with sand and TDA with height 1.5m and 4.5m

4.2.5 Validity of the scaled model

From fig 4.5, the concurrence between the results of the actual model and scaled – up model, is a clear indication that the model is valid. The scaled model validation provides confidence in the design and analysis of TDA backfilled retaining wall of larger heights, enabling the development of sustainable and resilient geotechnical infrastructure.

4.3 Influence of backfill slope and TDA layer width on retaining wall performance

The design of retaining wall backfilled with tire derived aggregate (TDA) requires careful consideration of various parameters to ensure optimal performance. This study now focuses on investigating the influence of backfill slope and the width of tire derived aggregate (TDA) layer on the performance of retaining wall backfilled with TDA. This study utilizes finite element analysis software, PLAXIS 2D, to simulate various scenarios and analyze the behavior of TDA backfilled retaining walls under different backfill slope and TDA layer width conditions. Four different cases of backfill slope were considered here, 0°, 10°, 20° and 30° and six different subcases were studied here for the width of TDA layer, the first subcase was with no TDA layer and the backfill was only sand, from the second subcase onwards, TDA width varied as 0.3m, 0.6m, 0.9m, 1.2m and 1.5m. In total, 24 model sets were developed and analyzed in this study. The geometry of the retaining wall and the material properties in all these trials were set similar to the scaled-up model of retaining wall discussed previously in this chapter. The retaining wall was assumed to be rigid. The backfill on both sides of the wall were assumed to be at different elevations. A uniform surcharge was applied on top of the backfill on the back side of the

wall. The following table presents the work plan parameters in each case of varying backfill slope.

Table 4.2 Work plan parameters used in the parametric study

Backfill slopes	Dimensions	Backfill on front side of the RW	Backfill on back side of the RW	Surcharge applied
No slope	H=4.5m, BW=2.1m, T=0.36m	H=1m Sand backfill	No TDA only sand backfill	24.9kPa
Slope 10°				
Slope 20°				
Slope 30°				
No slope	H=4.5m, BW=2.1m, T=0.36m	H=1m Sand backfill	0.3m TDA and sand backfill	24.9kPa
Slope 10°				
Slope 20°				
Slope 30°				
No slope	H=4.5m, BW=2.1m, T=0.36m	H=1m Sand backfill	0.6m TDA and sand backfill	24.9kPa
Slope 10°				
Slope 20°				
Slope 30°				
No slope	H=4.5m, BW=2.1m, T=0.36m	H=1m Sand backfill	0.9m TDA and sand backfill	24.9kPa
Slope 10°				
Slope 20°				
Slope 30°				
No slope	H=4.5m, BW=2.1m, T=0.36m	H=1m Sand backfill	1.2 m TDA and sand backfill	24.9kPa
Slope 10°				
Slope 20°				
Slope 30°				
No slope		H=1m		

Backfill slopes	Dimensions	Backfill on front side of the RW	Backfill on back side of the RW	Surcharge applied
Slope 10°	H=4.5m, BW=2.1m, T=0.36m	Sand backfill	1.5 m TDA and sand backfill	24.9kPa
Slope 20°				
Slope 30°				

4.3.1 Finite Element Model (FEM)

- Case 1: No backfill slope (slope 0°)

The following figure 4.6 presents the geometry of the model with 0° slope angle.

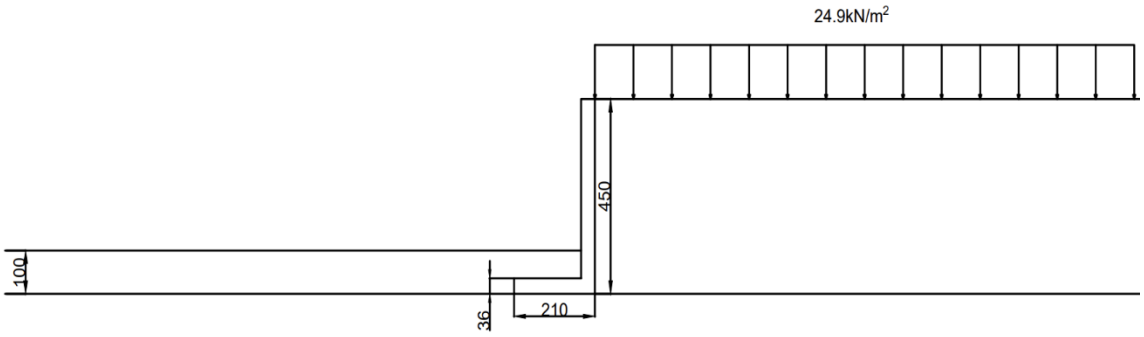

Fig 4.6 Geometry of retaining wall with no backfill slope

In the first subcase of this study, six different models were developed by varying with width of backfill TDA layer and studied. The backfill in each case was filled as three different layers, and the soil and TDA were backfilled separately. The following figures illustrates the developed model in each set in PLAXIS 2D.

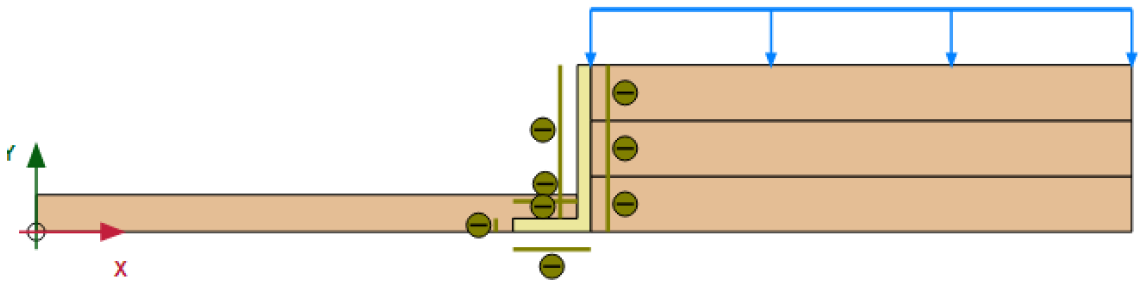

Fig 4.7 Retaining wall with no backfill slope and no TDA backfill

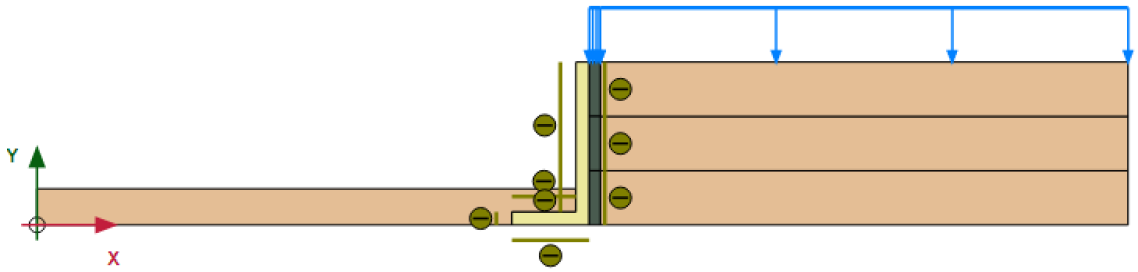

Fig 4.8 Retaining wall with no backfill slope and 0.3m width TDA backfill

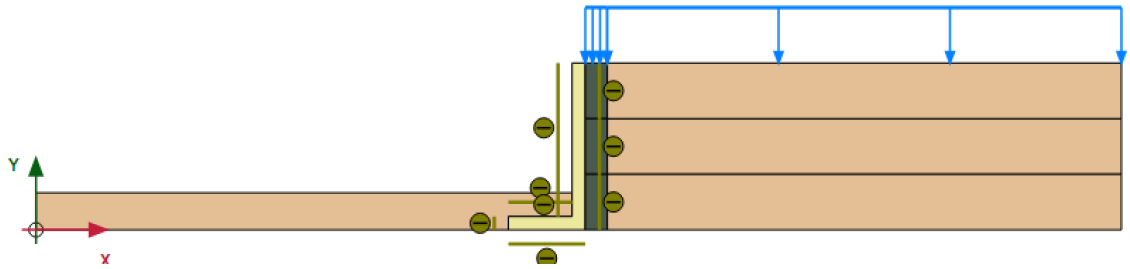

Fig 4.9 Retaining wall with no backfill slope and 0.6m width TDA backfill

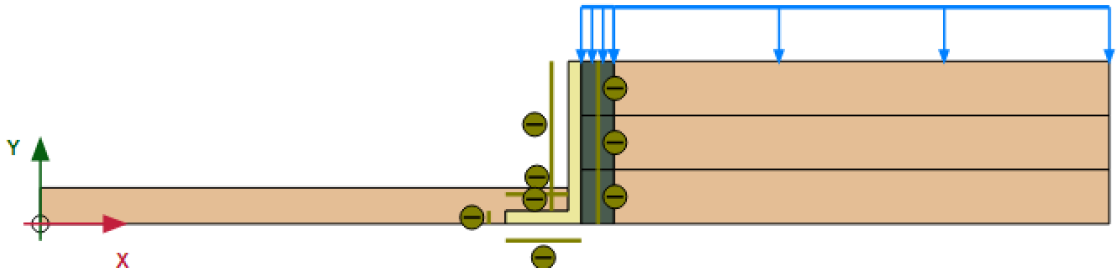

Fig 4.10 Retaining wall with no backfill slope and 0.9m width TDA backfill

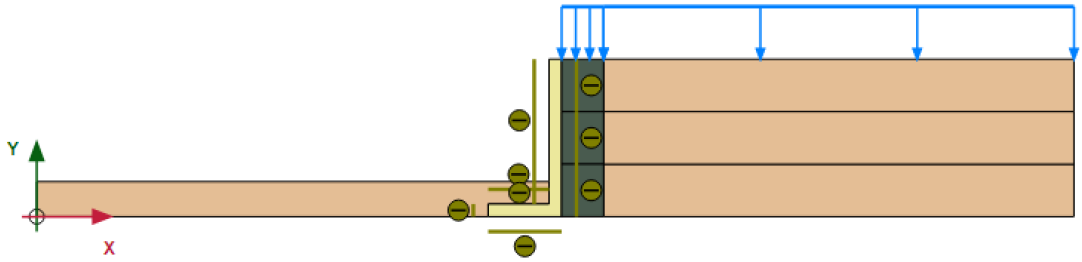

Fig 4.11 Retaining wall with no backfill slope and 1.2m width TDA backfill

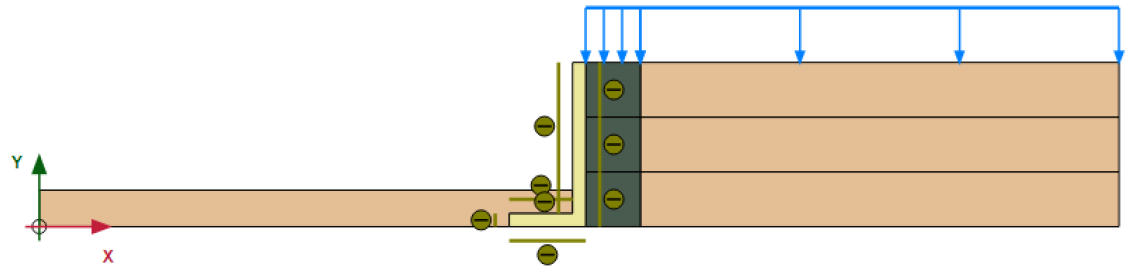

Fig 4.12 Retaining wall with no backfill slope and 1.5m width TDA backfill

- Case 2: Backfill slope of 10°

The following figure 4.13 presents the geometry of the model with 10° slope angle.

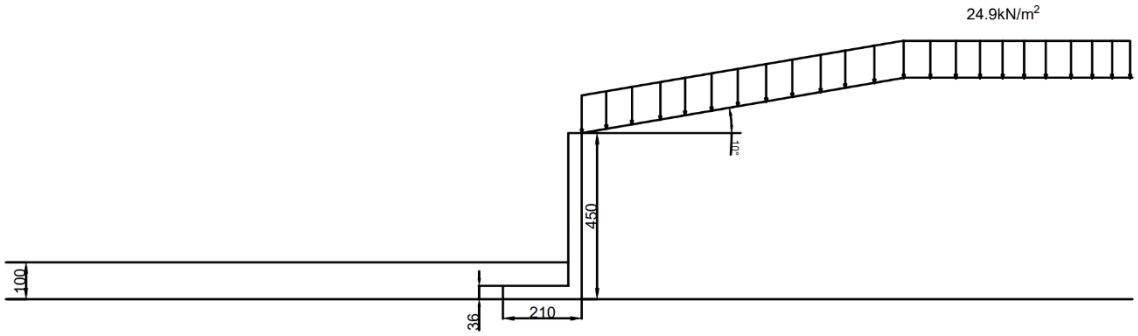

Fig 4.13 Geometry of retaining wall with backfill slope 10°

In the second case, backfill slope angle of 10° was given, and six different subcases were modeled by varying the width of backfill TDA layer in each subcase. The following figures illustrates the developed model in each set in PLAXIS 2D.

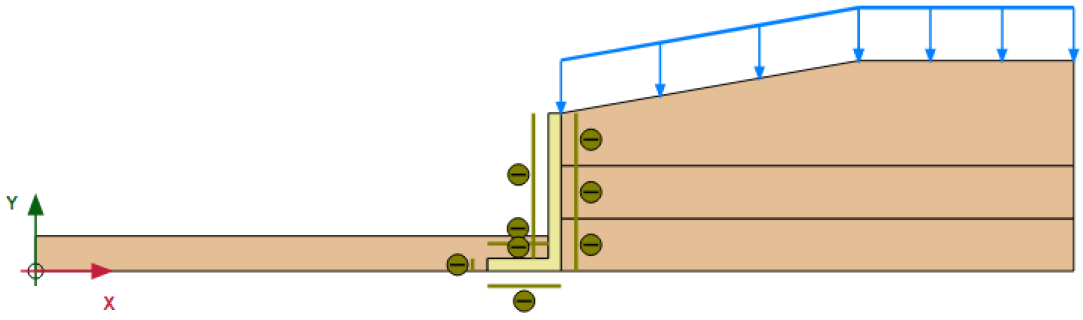

Fig 4.14 Retaining wall with backfill slope 10° and no TDA backfill

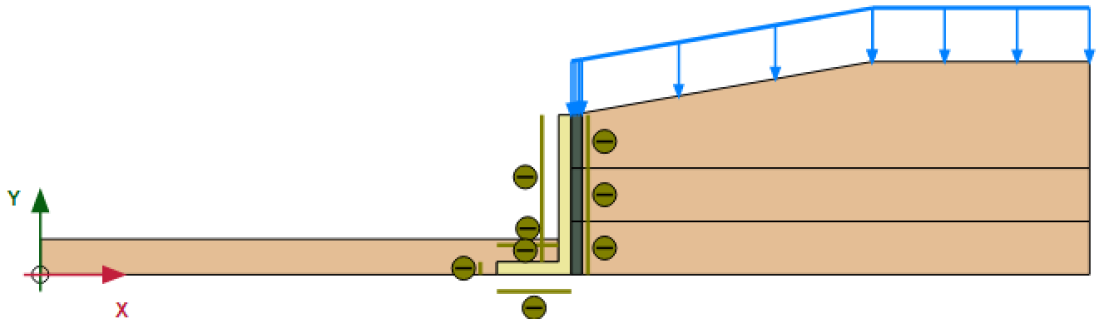

Fig 4.15 Retaining wall with backfill slope 10° and 0.3m TDA backfill

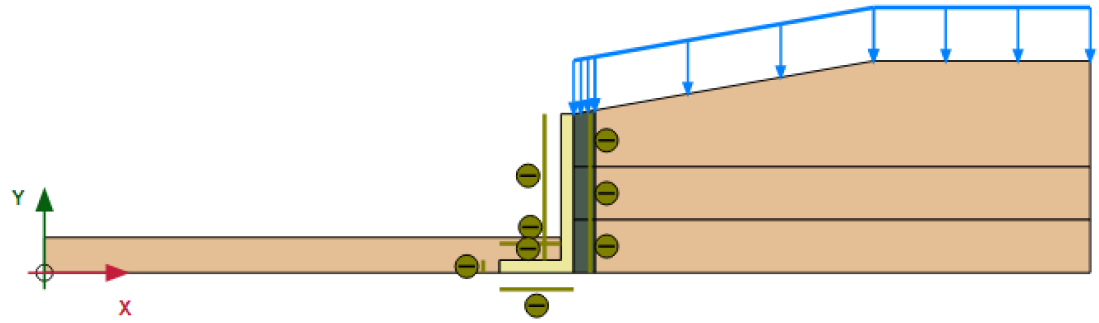

Fig 4.16 Retaining wall with backfill slope 10° and 0.6m TDA backfill

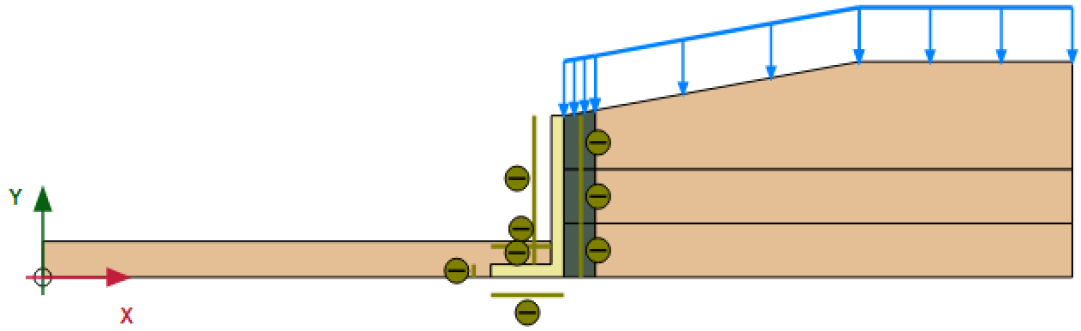

Fig 4.17 Retaining wall with backfill slope 10° and 0.9m TDA backfill

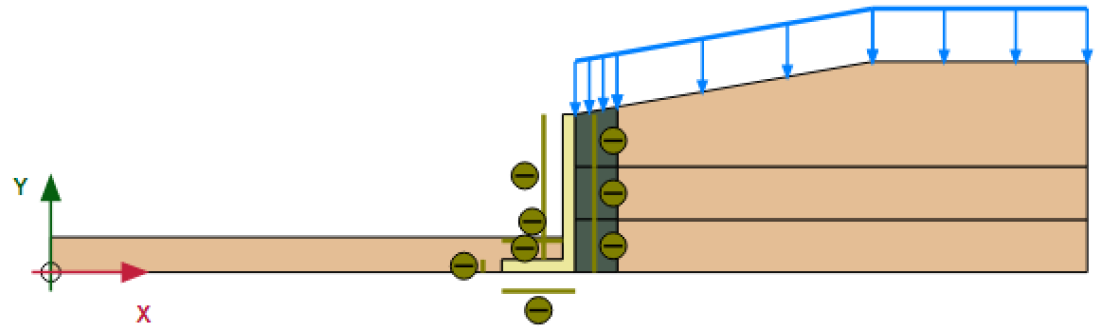

Fig 4.18 Retaining wall with backfill slope 10° and 1.2m TDA backfill

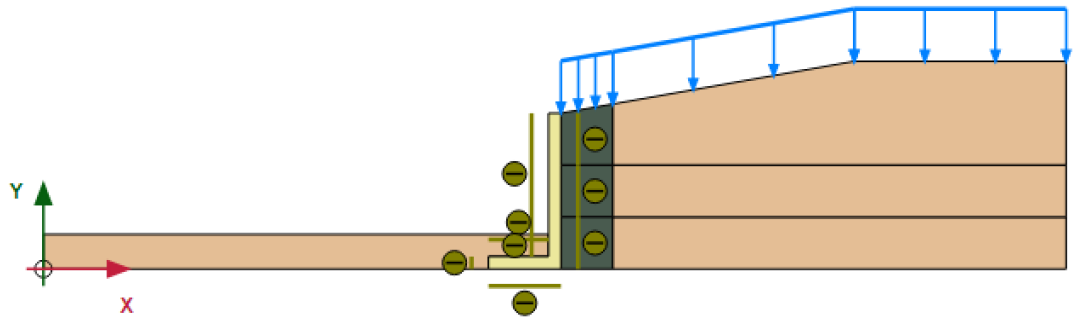

Fig 4.19 Retaining wall with backfill slope 10° and 1.5m TDA backfill

- Case 3: Backfill slope of 20°

The following figure 4.20 presents the geometry of the model with 20° slope angle. In the third set, backfill slope angle of 20° was given, and six different subcases were modeled by varying the width of backfill TDA layer in each subcase.

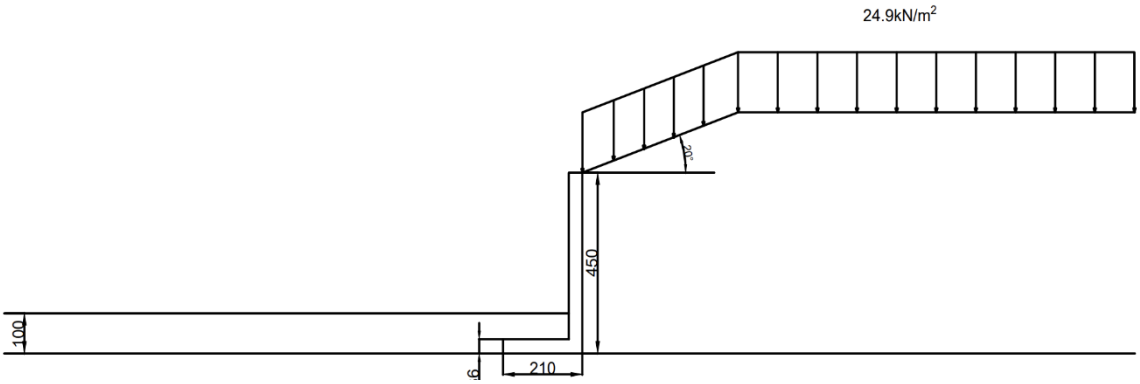

Fig 4.20 Geometry of retaining wall with backfill slope 20°

The following figures illustrates the developed model in each set in PLAXIS 2D.

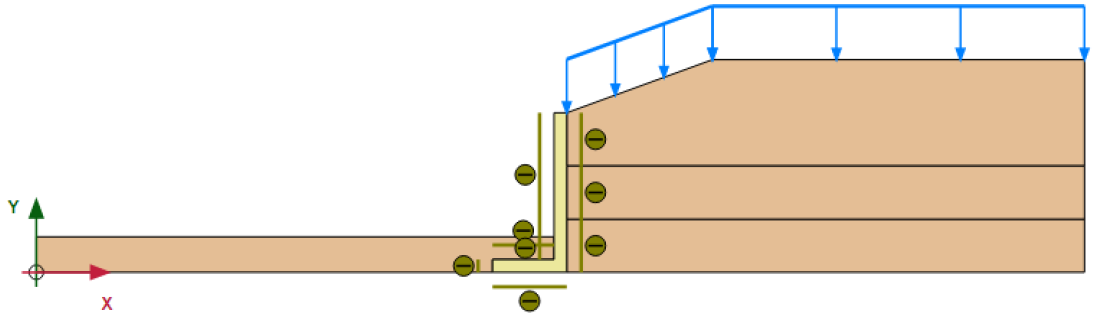

Fig 4.21 Retaining wall with backfill slope 20° and no TDA backfill

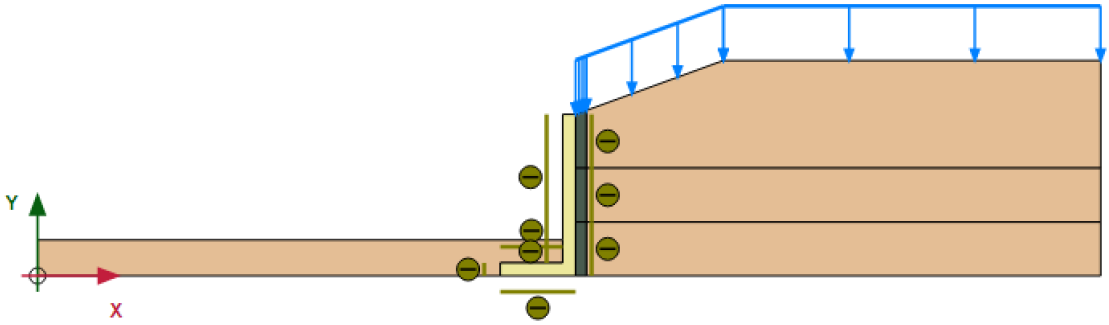

Fig 4.22 Retaining wall with backfill slope 20° and 0.3m TDA backfill

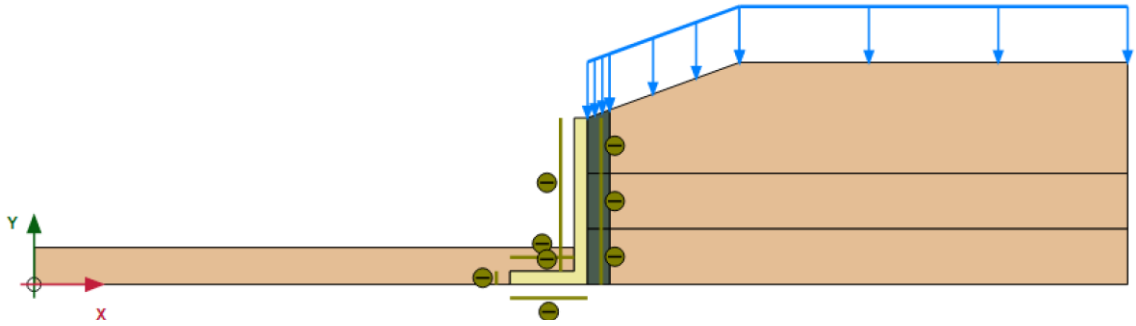

Fig 4.23 Retaining wall with backfill slope 20° and 0.6m TDA backfill

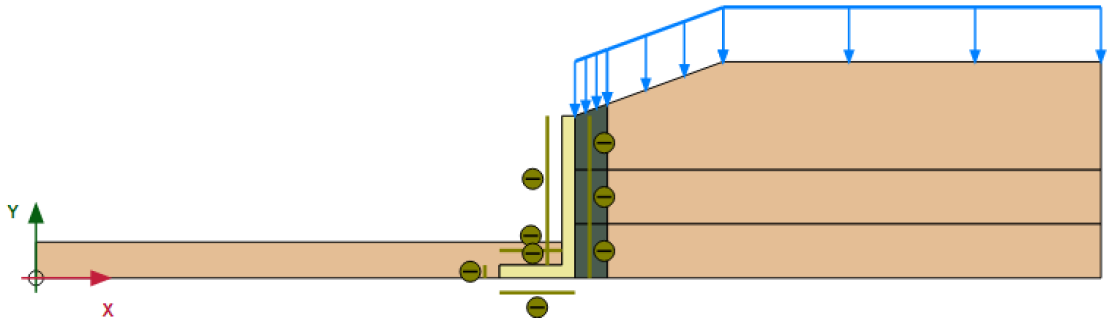

Fig 4.24 Retaining wall with backfill slope 20° and 0.9m TDA backfill

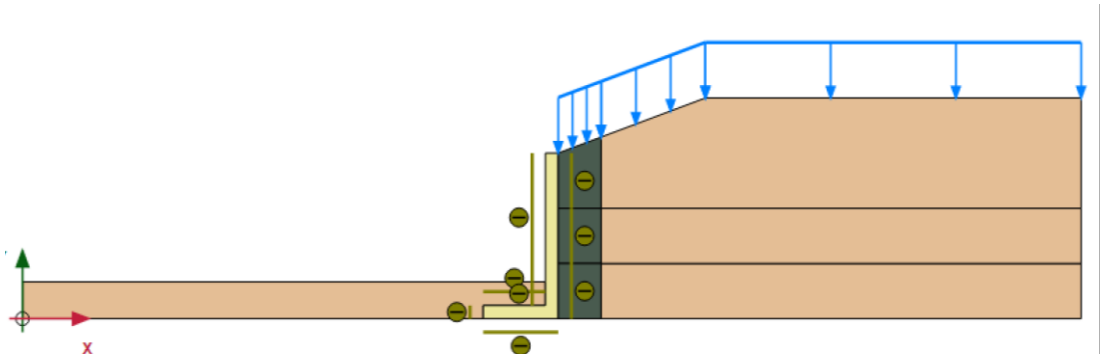

Fig 4.25 Retaining wall with backfill slope 20° and 1.2m TDA backfill

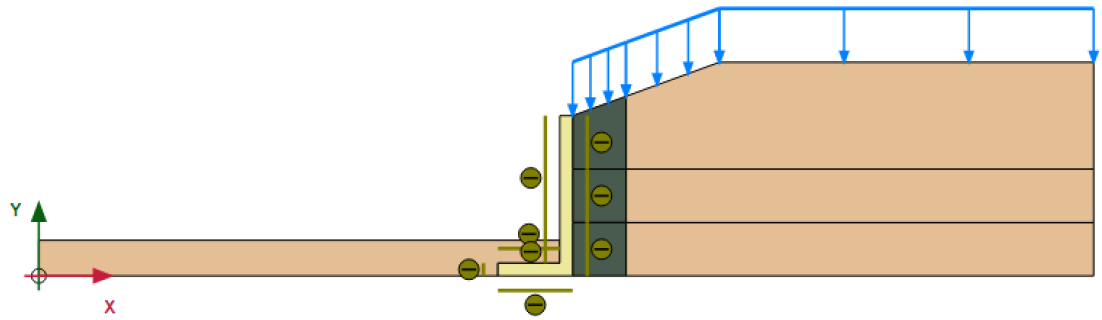

Fig 4.26 Retaining wall with backfill slope 20° and 1.5m TDA backfill

- Case 4: Backfill slope of 30°

The following figure 4.27 presents the geometry of the model with 30° slope angle.

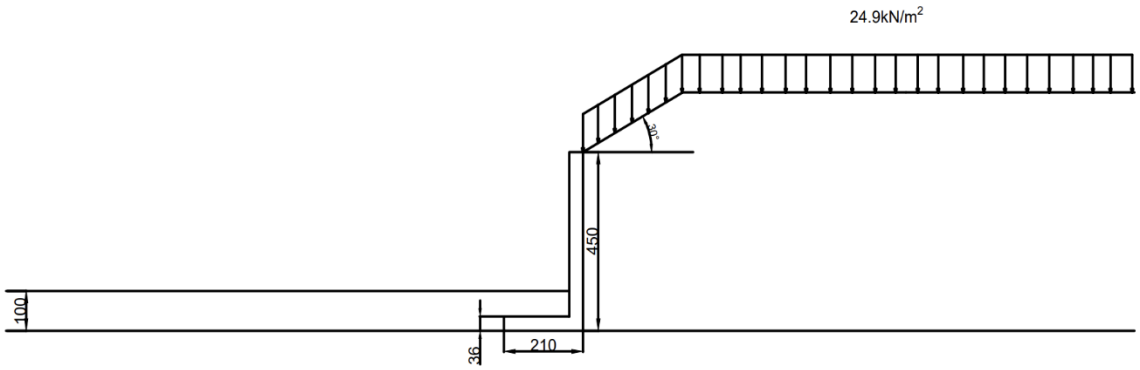

Fig 4.27 Geometry of retaining wall with backfill slope 30°

In the fourth set, backfill slope angle of 30° was given, and six different subcases were modeled by varying the width of backfill TDA layer in each case. The following figures illustrates the developed model in each set in PLAXIS 2D.

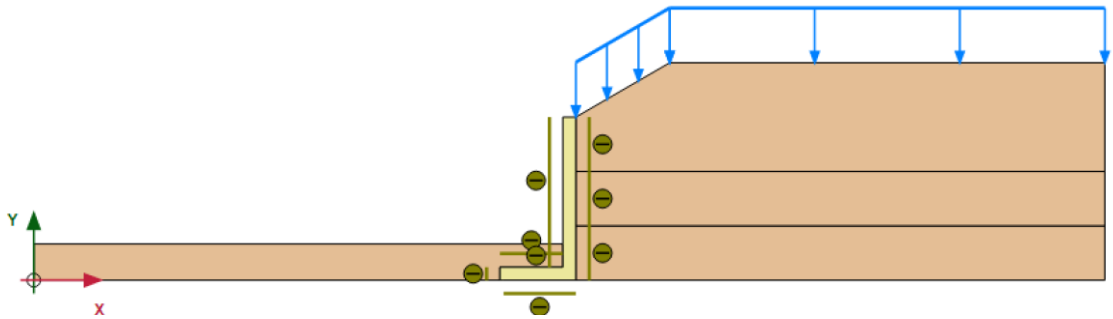

Fig 4.28 Retaining wall with backfill slope 30° and no TDA backfill

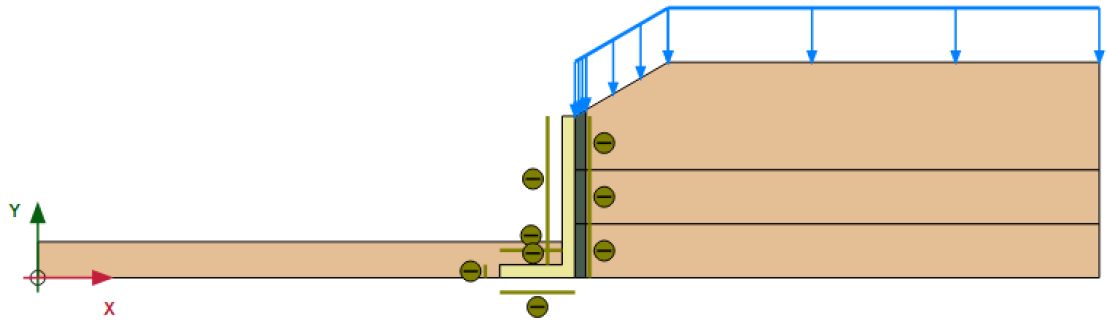

Fig 4.29 Retaining wall with backfill slope 30° and 0.3m TDA backfill

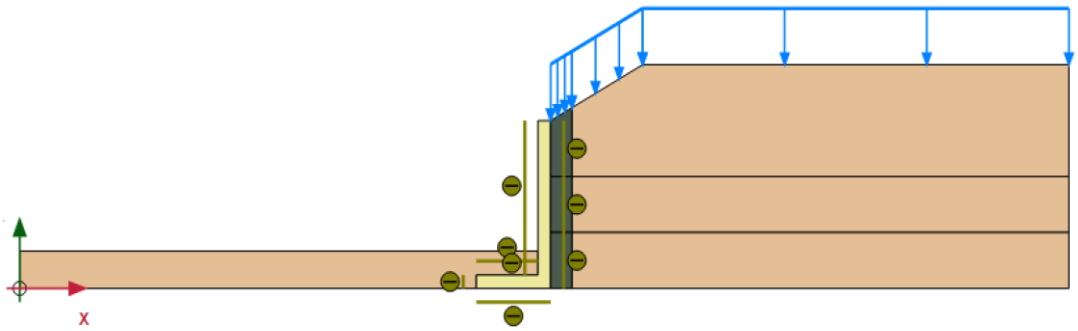

Fig 4.30 Retaining wall with backfill slope 30° and 0.6m TDA backfill

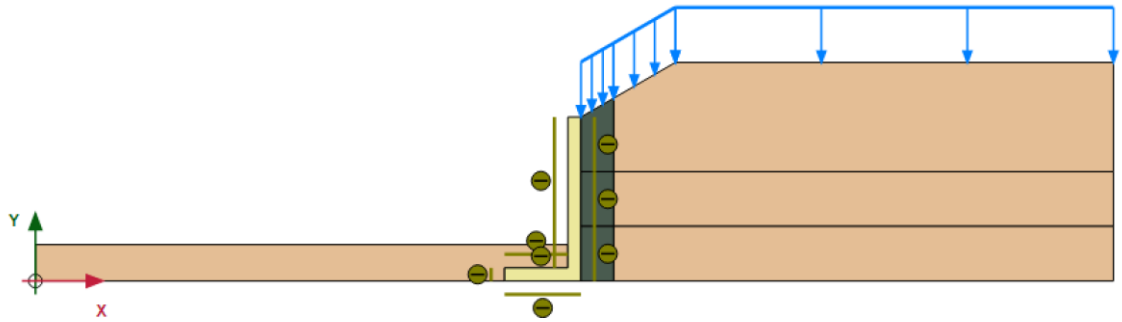

Fig 4.31 Retaining wall with backfill slope 30° and 0.9m TDA backfill

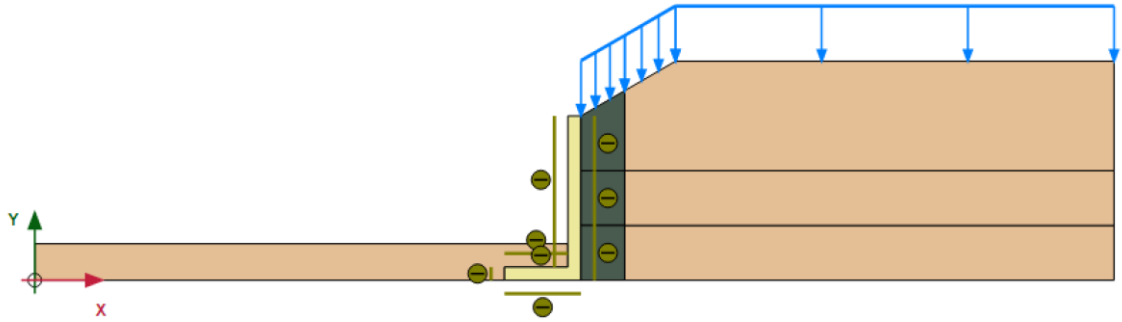

Fig 4.32 Retaining wall with backfill slope 30° and 1.2m TDA backfill

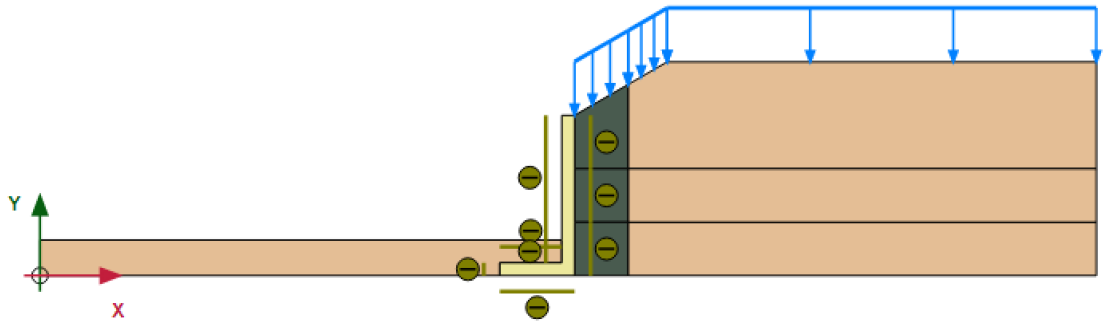

Fig 4.33 Retaining wall with backfill slope 30° and 1.5m TDA backfill

4.4 Results and Discussion

This section presents the findings of the parametric study on the behavior of retaining wall backfilled with Tire derived aggregate (TDA) under various conditions. The results reveal the effects of varying backfill slope and the width of backfill TDA layer on the earth pressure distribution. The discussion that follows interprets the results, highlights, key trends, and implications and compares the findings.

4.4.1 Earth pressure on retaining wall with no backfill slope

Earth pressure at various heights of the wall, 0.56m, 1.46m, 2.25m, 3.32m and 4.28m was studied for the comparison. It was observed that there is a reduction in earth pressure in the retaining wall as the width of TDA layer increases in each case. In the first subcase, where the retaining wall was backfilled with sand only, at the bottom of the wall at height 0.56m the earth pressure was found to be 21.20kPa, whereas as TDA was incorporated in the backfill, this was found to decrease slightly. For the second subcase where thickness of TDA backfill was 0.3m, at the same height the earth pressure was observed to be 7.39kPa. Whereas, as the width of TDA backfill increased in further subcases, slight decrease in earth pressure is further observed at the same height with lowest value of 5.85kPa for 1.5m thick TDA backfill. At the same time, at the bottom of the wall, though there was reduction in earth pressure it was comparatively lower than at the top of the wall, and it was found to be 3.65kPa for retaining wall backfilled with sand only at height 4.28m and 2.59kPa for retaining wall backfilled with 1.5m thick TDA backfill at the same height.

From the findings it can be concluded that tire derived aggregates are effective in reducing earth pressure slightly even at shallow slope angles. The following graph presents the earth pressure on the retaining wall in each case of varying width of TDA.

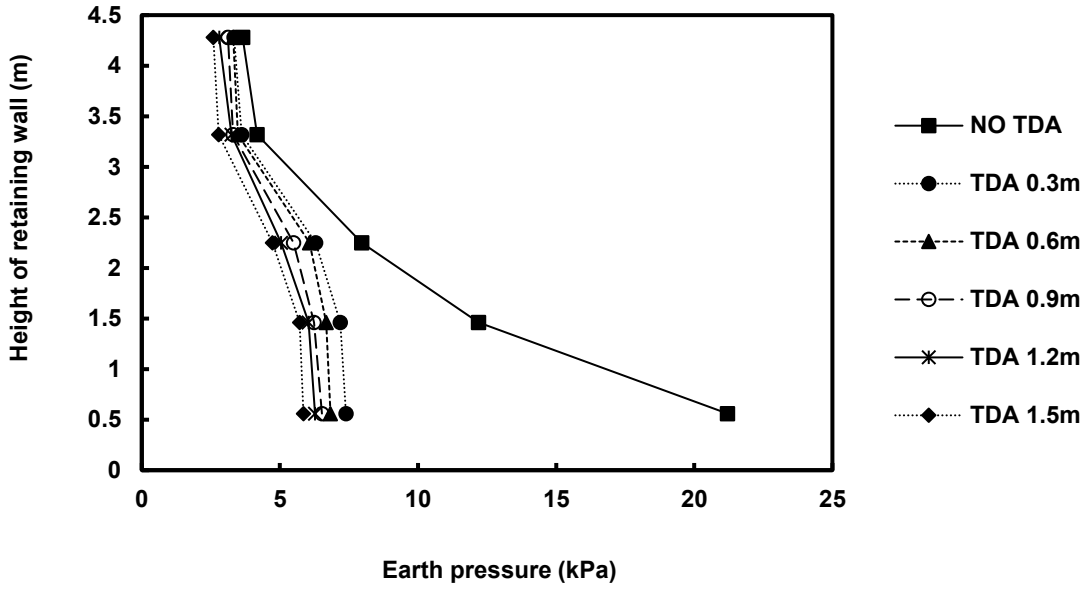

Fig 4.34 Earth pressure on retaining wall with no backfill slope

4.4.2 Earth pressure on retaining wall with backfill slope of 10°

Earth pressure at various heights of the wall, 0.56m, 1.46m, 2.25m, 3.32m and 4.28m was studied for the comparison. In the first subcase, where the retaining wall was backfilled with sand only, at the bottom of the wall at height 0.56m the earth pressure was found to be 23.71kPa, whereas as TDA was incorporated in the backfill, this was found to decrease

slightly. For the second subcase where thickness of TDA backfill was 0.3m, at the same height the earth pressure was observed to be 7.70kPa. Whereas, as the width of TDA backfill increased in further subcases, slight decrease in earth pressure is further observed with lowest value of 7.02kPa at the same height for 1.5m thick TDA backfill. At the same time, at the bottom of the wall, though there was reduction in earth pressure it was comparatively lower than at the top of the wall, and it was found to be 4.73kPa for retaining wall backfilled with sand only at height 4.28m and 2.91kPa for retaining wall backfilled with 1.5m thick TDA backfill at the same height. These findings demonstrates the potential of tire derived aggregate to improve the stability of retaining wall at moderate slope angles.

The following graph presents the earth pressure on the retaining wall in each case of varying width of TDA.

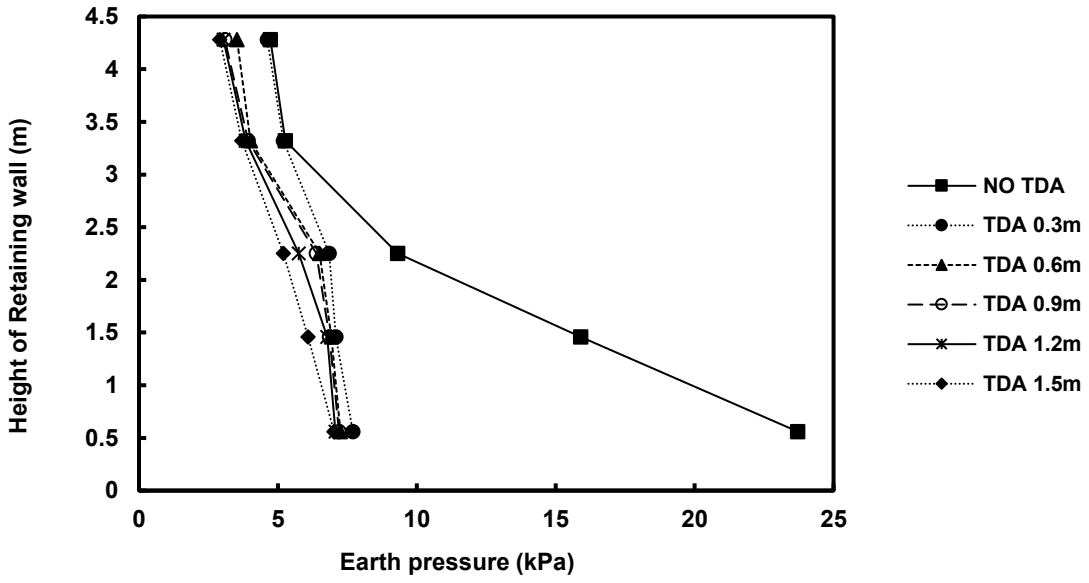

Fig 4.35 Earth pressure on retaining wall with backfill slope of 10°

4.4.3 Earth pressure on retaining wall with backfill slope of 20°

Earth pressure at various heights of the wall, 0.56m, 1.46m, 2.25m, 3.32m and 4.28m was studied for the comparison. In the first subcase, where the retaining wall was backfilled with sand only, at the bottom of the wall at height 0.56m the earth pressure was found to be 25.22kPa, whereas as TDA was incorporated in the backfill, this was found to decrease slightly. For the second subcase where thickness of TDA backfill was 0.3m, at the same height the earth pressure was observed to be 8.04kPa. Whereas, as the width of TDA backfill increased in further subcases, slight decrease in earth pressure is further observed with lowest value of 7.09kPa at the same height for 1.5m thick TDA backfill. At the same time, at the bottom of the wall, though there was reduction in earth pressure it was comparatively lower than at the top of the wall, and it was found to be 6.63kPa for retaining wall backfilled with sand only at height 4.28m and 2.37kPa for retaining wall backfilled with 1.5m thick TDA backfill at the same height. These findings indicate that TDA is effective even for structures built on sloping terrain, where stability is a major concern.

The following graph presents the earth pressure results in this case where the backfill slope was 20°.

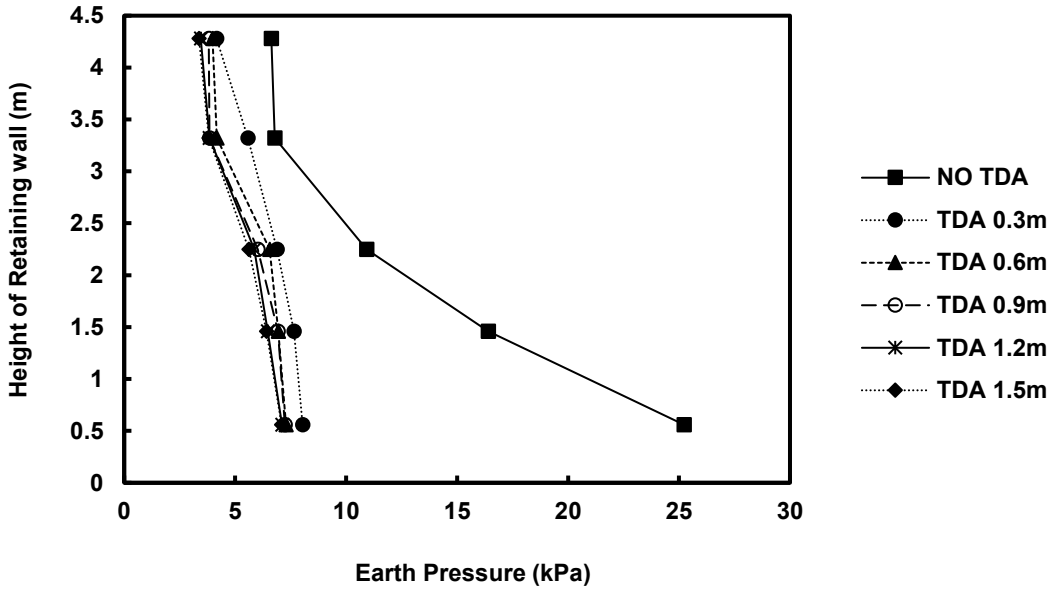

Fig 4.36 Earth pressure on retaining wall with backfill slope of 20°

4.4.4 Earth pressure on retaining wall with backfill slope of 30°

Earth pressure at various heights of the wall, 0.56m, 1.46m, 2.25m, 3.32m and 4.28m was studied for the comparison. In the first subcase, where the retaining wall was backfilled with sand only, at the bottom of the wall at height 0.56m the earth pressure was found to be 26.22kPa, whereas as TDA was incorporated in the backfill, this was found to decrease slightly. For the second subcase where thickness of TDA backfill was 0.3m, at the same height the earth pressure was observed to be 8.76kPa. Whereas, as the width of TDA backfill increased in further subcases, slight decrease in earth pressure is further observed with lowest value of 7.12kPa at the same height for 1.5m thick TDA backfill. At the same time, at the bottom of the wall, though there was reduction in earth pressure it was

comparatively lower than at the top of the wall, and it was found to be 6.79kPa for retaining wall backfilled with sand only at height 4.28m and 3.60kPa for retaining wall backfilled with 1.5m thick TDA backfill at the same height.

The following graph presents the earth pressure on the retaining wall in each case of varying width of TDA.

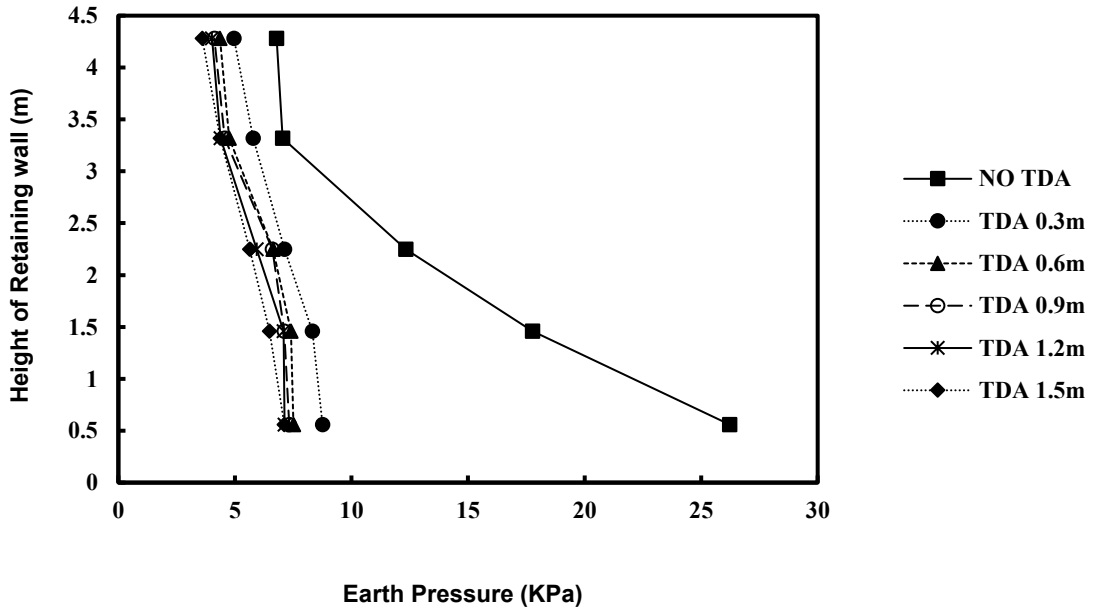

Fig 4.37 Earth pressure on retaining wall with backfill slope of 30°

4.4.5 Influence of backfill slope angle

From the findings mentioned in the previous sections, it was observed that varying backfill slope angle have only negligible effects on the earth pressure in the retaining wall. To confirm that, two graphs were plotted comparing the earth pressure in the retaining wall at the bottom at height 0.56m and at the top of height 4.28m, for all cases of backfill slop angle (0°,10°, 20° and 30°) where the retaining wall was backfilled without TDA and 0.3m thick TDA backfill.

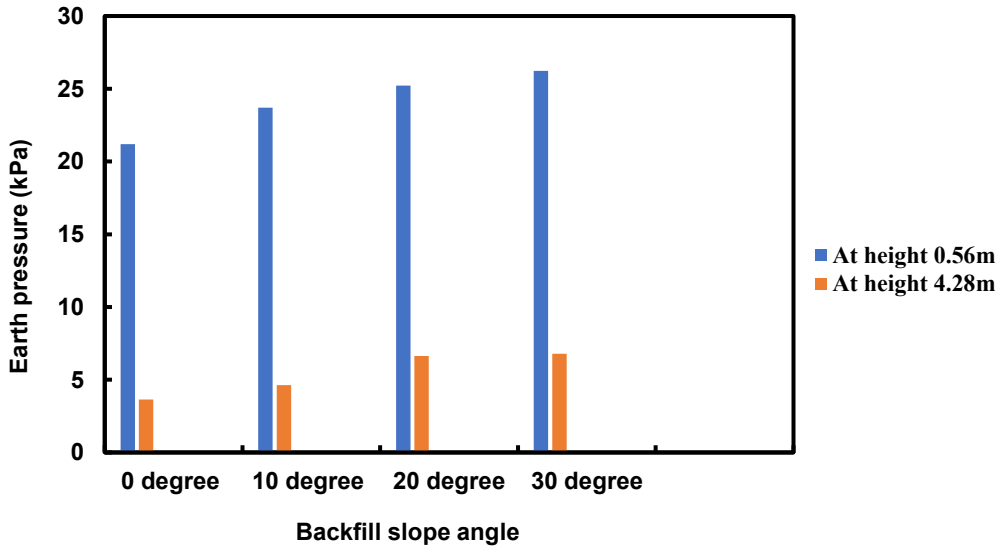

Fig 4.38 Earth pressure on retaining wall without TDA backfill at different slope angles

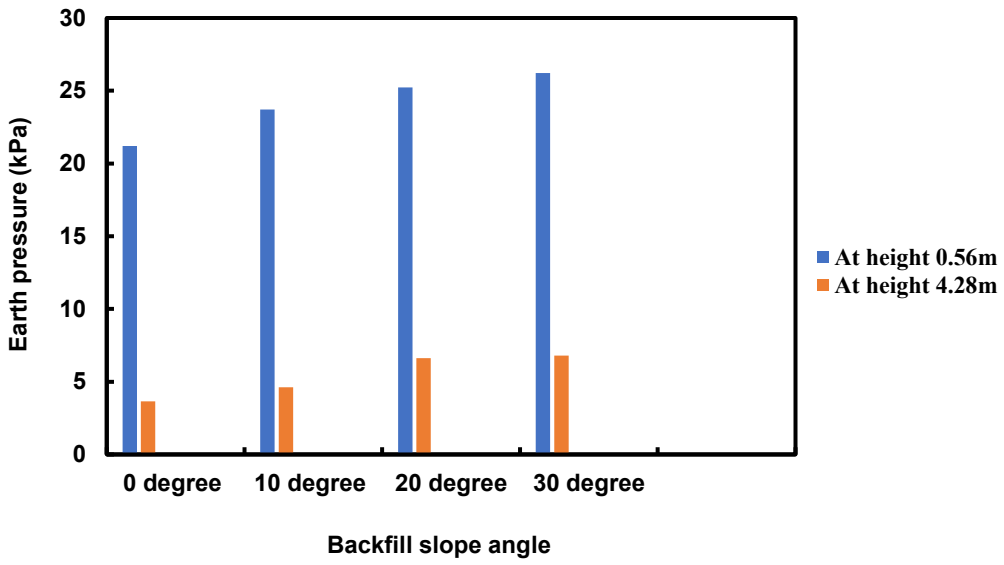

Fig 4.39 Earth pressure on retaining wall with 0.3m TDA backfill at different slope angles

4.4.6 Discussion

The study reveals a significant reduction in earth pressure, when TDA was introduced as a backfill material. The result from the parametric study clearly indicates that the earth pressure in the retaining wall significantly decreases with the increase of the width of TDA layer. The highest earth pressure in retaining wall was observed when the wall was backfilled with sand only and not TDA. However, in the following cases where retaining wall was backfilled with TDA and sand, different width of TDA layer was studied (0.3m, 0.6m, 0.9m, 1.2m and 1.5m). From the analysis, it can be concluded that, increasing the width of TDA layer in retaining walls effectively reduces the earth pressure and the 1.5m TDA layer was found to have the maximum reduction of earth pressure. Moreover, the

study showed that varying the backfill slope angle have only negligible effect on the results.

4.5 Conclusion

This chapter presented the results of a comprehensive investigation into the behavior of TDA backfilled retaining wall using PLAXIS 2D software on a series of parametric studies. This chapter investigated the validity of a scaled – up model of a retaining wall, and the behavior of TDA backfilled retaining wall under various slope angles and TDA layer widths. The following conclusions were made:

- The validity check revealed the accuracy and reliability of the scaled – up model, for subsequent parametric studies.
- The increase in slope angle from 0° to 30° have only negligible effect in the earth pressure on the retaining wall.
- The width of TDA layer has a profound impact on earth pressure reduction on retaining wall.

These findings have significant implications for geotechnical design, highlighting the potential and benefits of TDA as a sustainable backfill material in retaining wall construction.

CHAPTER 5 CONCLUSION AND RECOMMENDATIONS

5.1 Conclusion

This research has demonstrated the potential of Tire-Derived Aggregate (TDA) as a sustainable backfill material for retaining wall. Cost effectiveness, enhanced safety, improved drainage, long – term durability, reduced earth pressure and environmental benefits makes TDA a better substitute that normal conventional backfill materials. 2D finite element analysis (FEA) was carried out using PLAXIS 2D software.

In Chapter 3, a field test experiment conducted by Hazarika (2005) was used for the study. A 2D finite element model was developed using PLAXIS 2D software with the same parameters used in the case study. Two retaining walls were modeled here, one backfilled with sand on both sides of the wall and a uniform surcharge on top, whereas the other wall with sand backfill on one side and a TDA layer sandwiched between wall and backfill on the other side and a uniform surcharge on top on either side of the wall. Sand was modeled as Mohr-Colomb model, TDA as Hardening Soil model (HS) and Linear Elastic Model was adopted for concrete structure. Earth pressure on retaining walls in both the cases were analysed and compared with the field test experiment results and proved to be valid. The study concluded that, when tire derived aggregate is incorporated, a reduction in earth pressure is observed, as a result of the transitioning of backfill to active state. When three beneficial properties of TDA like, light unit weight, small stiffness and small Poisson's ratio are incorporated, the backfill soil easily approaches active state, and hence reduction in earth pressure against the wall can be observed.

Chapter 4 presented a comprehensive parametric study on the behavior of a scaled – up retaining wall model backfilled with TDA. A 2D finite element model was developed using PLAXIS 2D software and the earth pressure on the wall was analyzed. Normalized stress of the actual model and the scaled model was compared, and it was found to be valid and suitable for subsequent parametric studies. Furthermore, various parametric studies were conducted on retaining wall backfilled with TDA under various slope angles and TDA layer widths. Four different cases of slope angle were considered, no slope, 10-degree slope, 20-degree slope and 30-degree slope. Under each case, different trial models were analysed by varying the width of TDA layers as no TDA layer, 0.3m TDA, 0.6m TDA, 0.9m TDA, 1.2m TDA and 1.5m TDA. Earth pressure on retaining walls in all these cases were analysed and compared. The study concluded that slope angle have negligible effect on earth pressure on retaining wall whereas, increasing the width of TDA layer effectively reduces the earth pressure and the 1.5m TDA layer was found to have the maximum reduced earth pressure.

5.2 Recommendations

- Experimental Validation: Experimental tests can be conducted to validate the numerical findings to enhance the understanding of TDA backfilled retaining walls.
- Long-term performance: Investigations can be carried out on the long-term behavior of TDA backfilled retaining wall under various environmental conditions.

- Seismic Analysis: Seismic Analysis can be conducted to evaluate the performance of TDA backfilled retaining wall under earthquake loads.
- Cost-benefit Analysis: Studies can be carried out to conduct a cost-benefit analysis to compare the economic validity of TDA backfilled retaining walls with traditional backfill materials.

REFERENCES

- ACI Code – 318-19. (2022). *Building Code Requirements for structural concrete and commentary*, American Concrete Institute.
- Ahn, I.S., Cheng, L., Fox, P.J., Wright, J., Patenaude, S., & Fujii, B. (2014). *Material Properties of Large-Size Tire Derived Aggregate for Civil Engineering Applications*, Journal of Materials in Civil Engineering, Vol.21, No. 9.
- Ahn, I.S., & Cheng, L. (2014). *Tire Derived Aggregate for retaining wall backfill under earthquake loading*, Construction and Building Materials Journal, Vol.57, 105-116.
- Ahn, I.S., & Cheng, L. (2017). *Seismic Analysis of semi-gravity RC cantilever retaining wall with TDA backfill*, Frontiers of Structural and Civil Engineering, Vol.11, 455-469.
- Ajayi, O., Okeke, O.C., Okonkwo, S.I., Fagorite, V.I., & Amadi, C.C. (2023). *Analysis of Earth Pressures and Stability of Retaining Walls; Review of Principles and Practices in Engineering Construction*, International Journal of Engineering and Modern Technology, Vol.9, 42-56.
- Amirkhanian, A., & Skelton, E. (2021). *Tire-derived aggregate applications in civil engineering*, Tire waste and recycling, 565-578.
- Anand, V., & Kumar, S.S.R. (2018). *Seismic Soil-structure Interaction: A State-of-the-Art Review*, Structures (16), 317-326.
- ASTM D6270. (2008). *Standard practice for Use of Scrap Tires in Civil Engineering Applications 1*.

- Arulrajah, A., Mohammadinia, A., Maghool, F., & Horpibulsuk, S. (2019). *Tire derived aggregates as a supplementary material with recycled demolition concrete for pavement applications*, Journal of Cleaner Production (230), 129-136.
- Benamara, F.Z., Rouaiguia, A., & Bencheikh, M. (2020). *Stability of Anchored Retaining wall under Seismic loading conditions to obtain minimum anchor lengths using the improved failure model*, Civil and Environmental Engineering Reports 30(3), 214-233.
- BIS Code. (2005). *Bureau of Indian Standards*, India.
- Boeckmann, A., & Loehr, J.E. (2017). *Design of Maintainable drains for earth retaining structures*, Institute for Transportation Iowa State University.
- Budhu, M. (2007). *Foundations and Earth Retaining Structures*, The University of California, 1-483.
- Cecich, V., Gonzales, L., Hoisaeter A., Williams, J., & Reddy, K. (1996). *Use of shredded tires as lightweight backfill material for retaining structures,* Waste Management Resources 14(5), 433-451.
- Cerminara, G., & Cossu, R. (2018). *Waste Input to Landfills*, Solid Waste Landfilling, 15-39.
- Cheng, D. (2016). *Usage Guide on Tire derived aggregate (TDA)*, California Department of Resources Recycling and Recovery, DRRR 2016-01545.
- Chowdhury, I., & Singh, J.P. (2013). *Performance evaluation of gravity type retaining wall under earthquake load*, Indian Geotechnical Journal, Vol. 44, 156-166.
- Craig, R.F. (1992). *Soil Mechanics Solutions Manual*, 35-48.

- Dagdeviren, U., & Kaymak, B. (2023). *Effect of the foundation soil properties on the optimum design of reinforced concrete retaining walls and defining critical boundary lines*, Vol.56.
- Damians, I.P., Bathurst, R.J., Lloret, A., Josa, A., & Mansouri, D.E. (2020). *Assessment of Earth Retaining Wall Sustainability: Value Functions and Stakeholder Weighting Sensitivity*, Sustainable Civil Infrastructures, 73-88.
- Das, B.M. (2019). *Principles of foundation Engineering*, Vol.7, 375-402.
- Dhamdhere, D.R., Rathi, V.R., & Kolase, P.K. (2018). *Design and Analysis of Retaining Wall*, International Journal of Management, Technology and Engineering, Vol.8, 1246-1263.
- Diaz, G., Herrera, R.F., Rivera, F.M-L., & Atencio, E. (2021). *Generative Design for Dimensioning of Retaining Walls*, MDPI Journal (09), 1918.
- Diwalkar, A. (2020). *Analysis and Design of Retaining Wall: A Review*, International Conference on Communication and Information Processing, Aissms IOIT, Pune, India.
- Djadouni, H., Trouzine, H., Correia, G.A., & Miranda, T.F. (2018). *Life cycle assessment of retaining wall backfilled with shredded tires*, The International Journal of Life Cycle Assessment, Vol.24, 581-589.
- Eurocode 7. (1997). *Geotechnical Design*, European Committee for Standardization, 35-81.
- Fan, K., Liu, S.H., Cheng, Y.P., & Wang, Y. (2019). *Sliding stability analysis of a retaining wall constructed by soilbags*, Geotechnique Letters, Vol.9, 1-7.

- Farooq, M.A., Nimbalkar, S., & Fatahi, B. (2022). *Sustainable Applications of Tyre-Derived Aggregates for Railway Transportation Infrastructure*, MDPI Journal 14(18), 11715.
- Gandomi, A.H., Kashani, A.R., Roke, D.A., & Mousavi, M. (2015). *Optimization of retaining wall design using recent swarm intelligence techniques*, Engineering Structures, Vol.103, 72-84.
- Hazarika, H., Sugano, T., Yasui, K., Mae, Y., & Ejiri, A. (2005*). Rigid Retaining Structure with Artificial and Recycled Geomaterials as Sandwiched Cushion*, Symposium on Artificial Geomaterials, Fukuoka, Japan. 77–82.
- Hulagabali, A., Solanki, C.H., Dodagoudar, G.R., & Konnur, S. (2018). *Analysis of Mechanically Stabilised Earth (MSE) Retaining Wall using Finite Element and AASHTO Methods*, Journal of Engineering Technology, Vol.6, 139-150.
- Humphrey, D.N., & Swett, M. (2006). *Literature Review of The Water Quality Effects of Tire Derived Aggregate and Rubber Modified Asphalt Pavement*, A Study for the U.S. Department of Environmental Protection Agency, Dept. of Civil and Environmental Engineering, University of Maine, Orono, Maine.
- IBC Code. (2018). *International Building Code*, The International Code Council, Washington, DC.
- IS 4458. (1997). *Indian Standards Code*, India.
- Jasim, N., & Yaqoobi, A.A. (2016). *Optimum design of tied back Retaining wall*, Open Journal of Civil Engineering, Vol.6, 139-155.

- Kaneda, K., Hazarika, H., & Yamazaki, H. (2018). *Examination of earth pressure reduction mechanism using tire-chip inclusion in sandy backfill via numerical simulation*, Soils and Foundations, Vol.58, 1272-1281.
- Karkanaki, A.R., Ganjian, N., & Askari, F. (2017). *Stability Analysis and Design of Cantilever retaining walls with regards to possible failure mechanisms: An upper bound limit analysis approach*, Geotechnical and Geological Engineering Journal, Vol.35, 1079-1092.
- Khan, A.J., & Sikder, M. (2004). *Design basis and economic aspects of different types of retaining walls*, Journal of Civil Engineering, Vol.32, 17-34.
- Kong, S-M., Oh, W-D., Lee, S-Y., & Lee, Y-J. (2021). *Analysis of reinforced retaining wall failure based on reinforcement length*, International Journal of Geo-Engineering, Vol.12 (13).
- Kumar, A., & Parihar, A. (2023). *Design and Life Cycle Assessment of Retaining Wall with Used Foundry Sand as Backfill*, Construction and Building Materials Journal.
- Ling, H.I., Liu, H., & Mohri, Y. (2005). *Parametric Studies on the Behavior of Reinforced Soil Retaining Walls under Earthquake Loading*, Journal of Engineering Mechanics, Vol.131 (10).
- Longinos, M.J., & Widlund, J. (2022). An Article on Retaining Wall Design Process.
- Mahgoub, A., & El Naggar, H. (2019). *Using TDA underneath shallow foundations: simplified design procedure*, International Journal of Geotechnical Engineering, Vol.16, 787-801.
- Mazni, D.I., Hakam, A., Tanjung, J., & Anas, F. (2021). *Stability analysis of concrete block retaining wall based on a scaled laboratory*, Vol.331.

- Medina, B.M., Ordonez, J., Romana, M.G., & Galera, A.L. (2021). *Typology Selection of Retaining Walls Based on Multicriteria Decision-Making Methods*, MDPI Journal, Vol.11-1457.
- Olesiak, S., & Wisniewska, J.H. (2018). *Effectiveness of reinforcing an earth structure with a system of counterfort drains over a long-term use*, Vol.40 (4), 244-253.
- Orr, L.L.T. (2012). *How Eurocode 7 has affected geotechnical design- A review*, Trinity College, Dublin, Ireland.
- Park, J.K., DeNooyer, I.G., & Wahl, J.H. (2023). *State of Knowledge on the Effects of Tire-Derived Aggregate (TDA) Used in Civil Engineering Projects on the Surrounding Aquatic Environment*, MDPI Journal, Vol.15 (20)- 15141.
- *PLAXIS 2D Materials Model Reference Manual* (2021).
- *PLAXIS 2D Reference Manual* (2012).
- *PLAXIS 2D Reference Manual* (2021).
- Purkar, M.S., & Kute, S. (2015). *Finite element analysis of a concrete-rigid wall retaining a reinforced backfill*, International Journal of Geo-Engineering, Vol.6 (14).
- Reddy, S.B., & Krishna, A.M. (2015). *Recycled Tire Chips Mixed with Sand as Lightweight Backfill Material in Retaining Wall Applications: an Experimental Investigation*, International Journal of Geosynthetics and Ground Engineering, Vol.1 (31).
- Saikia, S.S., & Battacharjee, A. (2021). *Numerical Model Study of Two-Tiered Reinforced Soil Retaining Wall Subjected to Dynamic Excitation*, IGC, Vol.4, 921-929.

- Sanjei, C., & De Silva, L.I.N. (2015). *Effect of construction sequences on the behavior of gravity type retaining wall: A case study*, Vol.109, 1-7.
- Shehata, S. (2016). *Retaining walls with relief shelves*, Innovative Infrastructure solutions journal, Vol.1 (4).
- Shrawankar, G.K., & Gangwal, S. (2024). *Design and Analysis of retaining wall structures*, International Journal of Science, Engineering and Technology, Vol.12.
- Shrestha, S., & Ravichandran, N. (2018). *Performance of retaining wall backfilled with tire aggregate under static and dynamic loading conditions: conventional designs and finite element simulation*, International Journal of Geotechnical Engineering, Vol.15, 574-586.
- Sivapriya, S.V., Sudharasan, C., Suraj, R., & Abhinaya, K. (2020). *A Preliminary Comparative Study of Seepage Behaviour Behind Retaining Walls with Crumb Rubber and Geo-composite*, Civil and Environmental Engineering Reports, Vol.30, 171-184.
- Sridevi, J., & Garg, K.G. (1997). *Finite element analysis of a reinforced earth wall*, Indian Geotechnical Journal.
- Tweedie, J.J., Humphrey, D.N., & Sandford, T.C. (1997). *Full-Scale Field Trials of Tire Shreds as Lightweight Retaining Wall Backfill Under At-Rest Conditions*, Transportation Research Record.
- Uray, E., Carbas, S., Erkan, I.H., & Tan, O. (2019). *Parametric investigation for discrete optimal design of a cantilever retaining wall*, Challenge Journal of Structural Mechanics, Vol.5 (3), 108-120.

- Vijayakumar, S., Subhash, A.B., Sumant, T.P., Venkatesh, M.B., & Yallappa, L.K. (2015). *A Case Study on Static Stability Analysis of Retaining Wall at Dewarwadi*, International Journal of Innovative Research in Science, Engineering and Technology, Vol.4, 3071-3077.
- Wang, Y., Zhang, X., Zhang, D., Fu, G., & Dong, X. (2022). *The structure design of integrated urban drainage systems: A view of robust optimization*, Journal of Environmental Management, Vol.322.
- Xiao, M., Bowen, M., Graham, M., & Larralde, J. (2012). *Comparison of Seismic responses of geo-synthetically reinforced walls with Tire derived aggregates and granular backfills*, Journal of Materials in Civil Engineering, Vol.24, 1368-1377.
- Zastrow, P., Moreno, F.M., Segura, T.G., Marti, J.V., & Yepes, V. (2017). *Life cycle assessment of cost-optimized buttress earth-retaining walls: A parametric study*, Journal of Cleaner Production, Vol.140 (03), 1037-1048.